

# Discrete turn strategies emerge in information-limited navigation

Jose M. Betancourt,<sup>1</sup> Matthew P. Leighton,<sup>1</sup> Thierry Emonet,<sup>1,2</sup> Benjamin B. Machta,<sup>1</sup> and Michael C. Abbott<sup>1</sup>

<sup>1</sup>*Department of Physics and Quantitative Biology Institute, Yale University, New Haven, CT, USA*

<sup>2</sup>*Molecular, Cellular, and Developmental Biology, Yale University, New Haven, CT, USA*

(Dated: 26 February 2026)

Navigation up a sensory gradient is one of the simplest behaviours, and the simplest strategy is run and tumble. But some organisms use other strategies, such as reversing direction or turning by some angle. Here we ask what drives the choice of strategy, which we frame as maximising up-gradient speed using a given amount of sensory information per unit time. We find that, without directional information on which way to turn, behavioural strategies which make sudden turns perform better than gradual steering. We see various transitions where a different strategy becomes optimal, such as a switch from reversing direction to fully re-orienting tumbles as more information becomes available. And, among more complex re-orientation strategies, we show that discrete turn angles are best, and see transitions in how many such angles the optimal strategy employs.

## Introduction

Many micro-organisms navigate by switching between a small set of discrete behavioural states in response to continuous changes in their sensory input. Run and tumble is one such strategy, alternating between swimming as straight as possible, and suddenly picking a new direction at random [1]. Other organisms swim backwards and forwards [2], or make right-angle turns [3]. Why do they do this, instead of making continuous changes? And how do they choose which such strategy to adopt? Here, we explore these questions by asking for the strategy that maximises speed up a gradient with a given sensory input. We use the information rate from heading to behaviour as a way to abstract away details of the sensor, to allow us to compare quite different strategies.

In the simplest organisms, such as *E. coli*, forward swimming produces a rate of change of the observed concentration of some attractant, which influences the internal chemical state, which in turn controls motors driving the flagella. The noise in every step of this process limits how much information flows from heading to behaviour. Focusing on the end-to-end information rate gives us a framework in which to study what is in principle possible, which applies equally to quite different systems. However, it will be important to make a distinction between directional information and the non-directional kind collected by *E. coli*. While both are measured in bits per second, knowing which way to steer is qualitatively different, and changes what strategies are possible.

What we find is that if the sensor does not provide directional information, then continuous steering is always worse than sudden changes. As the amount of sensory information varies, for instance because the gradient steepness changes, we see various transitions of which strategy is best. Further, if we allow arbitrary actions, then the optimal strategy employs a discrete set of turn angles. These results are an example of how discreteness emerges from optimisation with limited information.

For simplicity we start with navigation in two dimensions, with an agent swimming at some fixed speed  $v_0$ , and able to sense some information about the angle  $\theta$

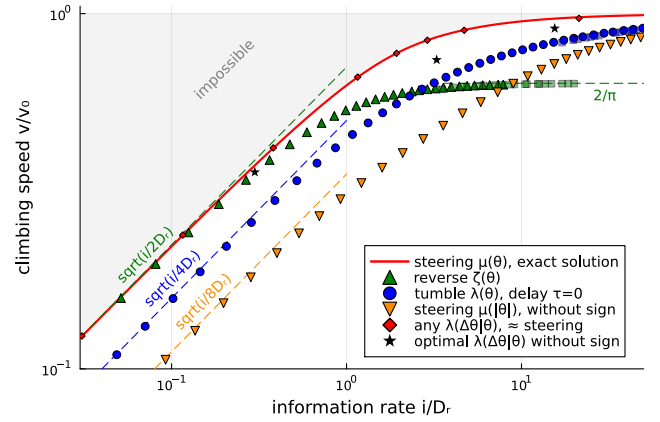


**Figure 1:** Performance of strategies for two-dimensional navigation, on the speed-information plane. The continuous steering strategy achieves the highest performance, provided the sign of heading  $\theta$  is visible (red). Among strategies not using the sign, fully re-orienting instantaneous tumbles (blue) perform well at high information rates, but at lower rates reversing (green) needs half as much information for the same speed. All low-information limits are  $v \sim \sqrt{i}$ , and high-information limits  $v/v_0 \rightarrow 1$  except reverse, which is limited to  $v/v_0 < 2/\pi \approx 0.64$ . Plot points are numerical, and square points (blue & green) use ansatz  $\lambda_{\text{strong}}(\theta)$ . Black stars are from figure 3.

away from straight uphill. This angle suffers rotational diffusion  $D_r$ , which tends to randomise the heading in time of order  $1/D_r$ . The noise from diffusion must be counteracted by a control system, which we model as a map from the present heading  $\theta$  to the controlled portion of the change of heading,  $d\theta_c$ . Then we ask for the control strategy which maximises mean climbing speed,  $v/v_0 = \langle \cos \theta \rangle_\theta$ , at a given rate of information,  $i = I(\Theta; d\Theta_c)/dt$ . We do so by introducing a trade-off parameter  $\gamma > 0$ , to arrive at the following optimisation problem:

$$\max_c (v/v_0 - \gamma i). \quad (1)$$

Finding the optimal control strategy  $c$  for many different values of  $\gamma$  gives us a frontier on the speed-information plane. We do this for various classes of control strategy, starting with the simplest.

### Steering vs. tumbling, in two dimensions

We begin by comparing two behaviours: *steering*, which continuously updates the heading at rate  $\mu$ , and *tumbling*, which picks a new heading at random with rate  $\lambda$ . We divide the evolution of the heading  $d\theta$  in time  $dt$  into a controlled part  $d\theta_c$  and Gaussian noise  $dW$  from diffusion:

$$\begin{aligned} d\theta &= d\theta_c + \sqrt{2D_r}dW \\ d\theta_c &= \mu(\theta) dt + \Delta\theta dJ(\lambda(\theta)) + \sqrt{2D_c}dW'. \end{aligned} \quad (2)$$

Here  $dJ$  is a Poisson jump process,  $\Delta\theta \sim U(-\pi, \pi)$  is the change in heading after a tumble, and  $D_c$  is controller noise. The equivalent Fokker-Planck equation is

$$\begin{aligned} \frac{dp(\theta)}{dt} &= -\lambda(\theta)p(\theta) + \int \frac{d\theta'}{2\pi} p(\theta')\lambda(\theta') \quad (\text{tumbling}) \\ &\quad - \frac{d[\mu(\theta)p(\theta)]}{d\theta} + (D_c + D_r)\frac{d^2p(\theta)}{d\theta^2} \quad (\text{steering \& noise}). \end{aligned}$$

Given the description of the strategy by  $\lambda(\theta)$ ,  $\mu(\theta)$  and  $D_c$ , we can solve  $dp(\theta)/dt = 0$  to obtain the steady-state distribution. This distribution  $p(\theta)$  can be viewed as a population average, or the long-time average of one individual. It allows us to compute the mean climbing speed,  $v/v_0 = \langle \cos \theta \rangle_\theta = \int d\theta p(\theta) \cos \theta$ .

The information rate we use is mutual information between the heading  $\theta$  and the controlled update  $d\theta_c$ , per time  $dt$ . For tumbling alone, this is

$$i = I(\Theta; d\Theta_c)/dt = \left\langle \lambda(\theta) \log \frac{\lambda(\theta)}{\langle \lambda(\theta') \rangle_{\theta'}} \right\rangle_\theta. \quad (3)$$

This form can be derived by considering the two possible actions,  $p(\text{tumble}|\theta) = \lambda(\theta)dt$  and  $p(\text{run}|\theta) = 1 - \lambda(\theta)dt$ . The formula for continuous steering can be derived by allowing small steps left or right of angle  $\pm\alpha$  at rates  $\beta_\pm(\theta) = D_c/\alpha^2 \pm \mu(\theta)/2\alpha$ . We give more detail (and another approach) in the appendix, but the result is an information rate proportional to the variance of  $\mu(\theta)$ :

$$i = \left\langle [\mu(\theta) - \langle \mu(\theta') \rangle_{\theta'}]^2 \right\rangle_\theta / 4D_c \quad (4)$$

A steering strategy with very little controller noise is allowed, but the resulting large information rate is penalised by our objective, (1). Thus introducing  $D_c$  is a way to let our framework to model real processes in which little information flows from heading to action. Explicit controller noise is not needed for the tumble strategy, as the intrinsic noise of the Poisson process can play this role. That is, (3) can be made small by choice of  $\lambda(\theta)$  alone.

For tumbling, our setup is very similar to that used by Mattingly et. al. [4]. They drew a frontier on the

speed-information plane, at low information rates, and were able to experimentally place *E. coli* at about 70% of optimal performance, given the information they actually receive. In a shallow gradient, these bacteria receive around 1% of a bit per tumble. In this regime the tumble rate is only slightly modulated:

$$\lambda(\theta) = D_r \left[ 1 - \sqrt{4i/D_r} \cos \theta + \mathcal{O}(i/D_r) \right].$$

The resulting performance is  $v/v_0 \approx \sqrt{i/4D_r}$  for  $i \ll D_r$ . Here we assume that the turns are instantaneous, although real *E. coli* spend perhaps 10% of their time tumbling [5]. In the appendix we derive the effect of time penalty  $\tau$  per tumble on the solution.

In the opposite limit, when information is plentiful, our problem approaches the one studied by Strong et. al. [6]. They asked what strategy gives the fastest climbing, with a finite time penalty  $\tau$  per tumble, but no cost of information. They found a deterministic strategy: the agent should always tumble when  $|\theta| > \theta_{\text{thresh}}$ . To achieve high speed when tumbles are quick,  $\tau \ll 1/D_r$ , the threshold is low  $|\theta_{\text{thresh}}| \ll 1$ , describing a behaviour in which the agent tumbles many times in succession until landing on a nearly-uphill heading. Similar behaviour is seen in the solution to our problem with  $\tau = 0$  but a large finite information rate,  $i \gg D_r$ . We find that the following strategy, shown in figure 2A, is a reasonable approximation:

$$\lambda_{\text{strong}}(\theta) = \begin{cases} 0 & |\theta| < \theta_{\text{thresh}} \\ \lambda_{\text{max}} & \text{else.} \end{cases} \quad (5)$$

Turning now to study continuous changes of heading, we optimise both the steering rate  $\mu(\theta)$  and the controller noise  $D_c$ . The solution always has  $D_c = D_r$ , and it's possible to solve for  $\mu(\theta)$  exactly in terms of special functions. We give details in an appendix, but the leading term at low information rate is:

$$\mu(\theta) = -\sqrt{8iD_r} \sin \theta + \mathcal{O}(i/D_r).$$

This limit  $i \ll D_r$  has performance  $v/v_0 \approx \sqrt{i/2D_r}$ , and we plot the full curve on figure 1.

We see that the steering strategy has uniformly higher performance than tumbling. But an important difference is that it is exploiting the sign of  $\theta$ , in a way that tumbling could not. The optimal tumble rate is an even function,  $\lambda(\theta) = \lambda(|\theta|)$ , but the optimal  $\mu(\theta)$  is odd. A strategy in which the agent is always able to steer towards the correct direction may be relevant for a ship with a poor compass, or an organism large enough to sense the local gradient vector. But if the agent can only observe its rate of up-gradient motion — as for instance a ship measuring on the depth of water, or a bacterium sensing the rate of change of concentration — then it must be ignorant of the sign, and hence  $\mu(\theta)$  must be even.

We can impose this symmetry constraint when finding solutions. Without access to the sign, the performance of steering is worse than tumbling, as shown in figure 1

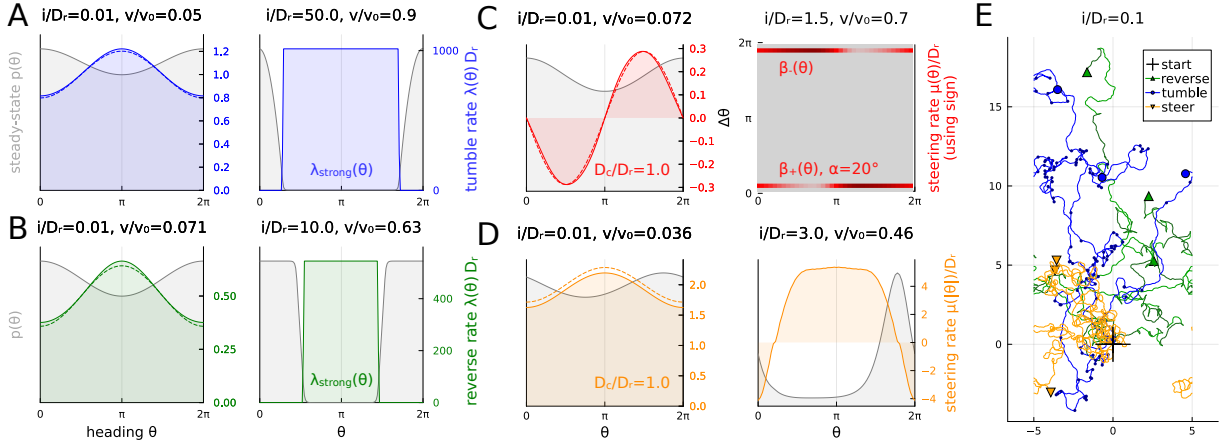


**Figure 2:** Numerical optimal strategies for run & tumble, steering, and reversing. (A) Tumble rate  $\lambda(\theta)$  in blue, and steady-state  $p(\theta)$  in grey, for a low-information case, and a high-information case using  $\lambda_{\text{strong}}(\theta)$ . (B) The reverse strategy achieves  $\sqrt{2}$  times the speed at similar information rate  $i/D_r \approx 0.01$ , by acting at half the rate of the tumble strategy. But its high-information case saturates at speed  $2/\pi$ , when  $p(\theta)$  is uniform on  $-\pi/2 \leq \theta \leq \pi/2$ . (C) Steering rate  $\mu(\theta)$  in red, and again  $p(\theta)$  in grey. Second panel translates  $\mu(\theta)$  and controller noise  $D_c = 1$  to  $\lambda(\Delta\theta, \theta)$  using two angles  $\Delta\theta = \pm\alpha$ . (D) Steering rate  $\mu(|\theta|)$ , assuming the sign of  $\theta$  is not observable. At low information rate, again  $i/D_r \approx 0.01$ , the agent always turns in one direction but modulates its turning speed. At high information rate, this strategy creates stable & unstable fixed points at some  $\pm\theta_*$ . (A-D) Dashed lines are analytic results at low information, from the text. (E) Sample trajectories for three strategies, all with  $i/D_r \approx 0.1$  (times  $0 < t < 50$  in units  $D_r = v_0 = 1$ , wrapped to  $-5 < x < 5$ ). More trajectories are shown in the appendix.

where the low-information limit is  $v/v_0 \approx \sqrt{i/8D_r}$  for  $i \ll D_r$ . The strategy here is to always turn in one direction, but slightly bias the rate:

$$\mu(|\theta|) = \pm 2D_r \left[ 1 - \sqrt{2i/D_r} \cos \theta + \mathcal{O}(i/D_r) \right].$$

At high information rates, the strategy is more interesting, see figure 2D. The optimal  $\mu(|\theta|)$  changes sign to create a pair of fixed points at  $\pm\theta_*$ , and the agent spends most of its time at whichever one is stable.

## Transitions between turn strategies

In the absence of directional information, we have seen that tumbles by  $\Delta\theta \sim U(-\pi, \pi)$  perform better than continuous steering. It is possible to do better by controlling the turn angle, and we will show that best strategy at low information rates is in fact to *reverse* direction,  $\Delta\theta = \pi$ . The Fokker-Planck equation for this strategy is

$$\frac{dp(\theta)}{dt} = -\lambda(\theta)p(\theta) + \lambda(\theta + \pi)p(\theta + \pi) + D_r \frac{d^2p(\theta)}{d\theta^2}$$

and the information rate is still (3). The optimal rate of reversal is at low information rates is

$$\lambda(\theta) = D_r/2 \left[ 1 - \sqrt{8i/D_r} \cos \theta + \mathcal{O}(i/D_r) \right].$$

This strategy uses half as much information for the same speed as tumbling:  $v/v_0 \approx \sqrt{i/2D_r}$  for  $i \ll D_r$ . But at high information, the best that it can do is to place all probability density within  $|\theta| < \pi/2$  (shown in figure 1B), leading to  $\langle \cos \theta \rangle_\theta = 2/\pi \approx 0.64$ . Hence figure 1 shows a

crossover: a transition between reverse and tumble being the best strategy, among the three not using the sign.

In the appendix we consider a *flick* strategy which uses right-angle turns,  $\Delta\theta = \pm\pi/2$ . This strategy beats both tumble and reverse in a medium-information regime (around  $i/D_r \approx 10$ ), but cannot exceed  $\langle \cos \theta \rangle_\theta = \sqrt{8}/\pi \approx 0.9$ . Thus we see two transitions between simple discrete strategies as the amount of information available increases.

## Discrete angles from arbitrary turns

Instead of a fixed turn angle  $\Delta\theta$  or a fixed distribution, we now look at the general case where  $\lambda(\Delta\theta, \theta)$  is the rate of initiating turns by  $\Delta\theta$  from heading  $\theta$ . All of the strategies already considered can be written as such a rate:

$$\lambda(\Delta\theta, \theta) = \begin{cases} \lambda(\theta)/2\pi & \text{tumble} \\ \delta(\Delta\theta - \pi) \lambda(\theta) & \text{reverse} \\ \delta(\Delta\theta - \alpha) \beta_+(\theta) + \delta(\Delta\theta + \alpha) \beta_-(\theta) & \text{steering.} \end{cases}$$

Here we use the same approximate translation of steering as above (4), and in figure 2C. The Fokker-Planck equation now reads

$$\frac{dp(\theta)}{dt} = \int d\phi \left[ \lambda(\theta - \phi, \phi)p(\phi) - \lambda(\phi, \theta)p(\theta) \right] + D_r \frac{d^2p(\theta)}{d\theta^2}$$

and the information rate is

$$i = \iint d\Delta\theta d\theta \lambda(\Delta\theta, \theta)p(\theta) \log \frac{\lambda(\Delta\theta, \theta)}{\bar{\lambda}(\Delta\theta)} \quad (6)$$

where  $\bar{\lambda}(\Delta\theta) = \int d\theta' \lambda(\Delta\theta, \theta')p(\theta')$ .

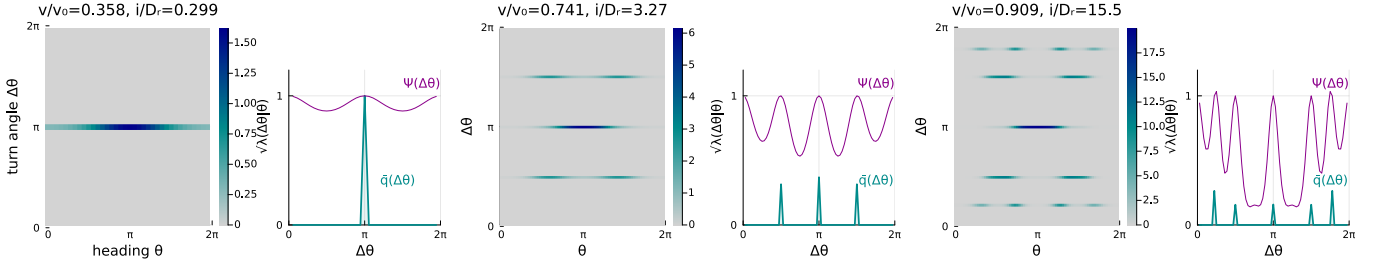


**Figure 3:** Discrete optimal strategies for three information rates. We impose that rate  $\lambda(\Delta\theta, \theta)$  is even in  $\Delta\theta$ , which implies that the strategy ignores the sign of  $\theta$ . At low information rate (left) we recover the reverse strategy,  $\Delta\theta = \pi$ , but with increasing information it bifurcates to use three angles (centre), and then five (right). Alongside the rate, we plot the contact function  $\Psi(\Delta\theta)$  and a mean distribution  $\bar{q}(\Delta\theta) \propto \bar{\lambda}(\Delta\theta)$ . The rate  $\lambda(\Delta\theta, \theta)$  is nonzero precisely where  $\Psi(\Delta\theta) = 1$ , but we do not allow turns of  $\Delta\theta = 0$ .

Solving numerically for the optimal  $\lambda(\Delta\theta, \theta)$ , we recover solutions equivalent to steering, which and are shown as red points on figure 1.

However, if we demand that the strategy be independent of the sign of  $\theta$ , then something more interesting happens, shown in figure 3. At low information rates, we recover the reverse strategy. But as more information becomes available, the solution bifurcates to use two additional angles,  $\Delta\theta \approx \pm\pi/2$ . With more information, it bifurcates again to use five angles, and so on, but the distribution of turn angles remains discrete.

To see why this discreteness emerges, we now formulate an augmented problem in which the Fokker-Planck equation  $dp(\theta)/dt = 0$  is imposed as a constraint, along with the symmetry  $\lambda(\Delta\theta, \theta) = \lambda(-\Delta\theta, \theta)$ , and the normalisation of  $p(\theta)$ . These are enforced by Lagrange multipliers: we maximise the following  $\mathcal{L}$  with respect to  $p, \lambda, \chi, \varphi, \xi$ :

$$\mathcal{L} = \langle \cos \theta \rangle_\theta - \gamma i + \int d\theta \chi(\theta) \frac{dp(\theta)}{dt} + \varphi \left[ 1 - \int d\theta p(\theta) \right] + \iint d\Delta\theta d\theta \xi(\Delta\theta, \theta) \left[ \lambda(\Delta\theta, \theta) - \lambda(-\Delta\theta, \theta) \right]$$

There are still two inequality constraints,  $p(\theta) \geq 0$ , and  $\lambda(\Delta\theta, \theta) \geq 0$ . This last constraint plays a crucial role, as the equation of motion  $\partial\mathcal{L}/\partial\lambda(\Delta\theta, \theta) = 0$  need only be satisfied where the constraint is slack,  $\lambda(\Delta\theta, \theta) > 0$ . After some algebra, this equation of motion reads

$$\lambda(\Delta\theta, \theta)/\bar{\lambda}(\Delta\theta) = e^{[\chi(\theta+\Delta\theta)+\chi(\theta-\Delta\theta)-2\chi(\theta)]/2\gamma}.$$

Taking the expectation value with  $p(\theta)$  on both sides leads to  $\Psi(\Delta\theta) = 1$ , where we define

$$\Psi(\Delta\theta) = \int d\theta p(\theta) e^{[\chi(\theta+\Delta\theta)+\chi(\theta-\Delta\theta)-2\chi(\theta)]/2\gamma}. \quad (7)$$

This contact function is analytic, and clearly has  $\Psi(0) = 1$ . Thus it must either be constant, or else have  $\Psi(\Delta\theta) = 1$  at a set of isolated points. In the appendix we show that  $\Psi''(0) = -\gamma i/D_r < 0$ , ruling out the constant case. Hence  $\lambda(\Delta\theta, \theta)$  is zero except at a discrete set of angles  $\Delta\theta$ . Figure 3 plots the contact function alongside the numerical

solutions  $\lambda(\Delta\theta, \theta)$  used to find it, for three information rates.

A similar construction without the symmetry constraint leads to the contact function being  $\Psi(\Delta\theta) = \int d\theta p(\theta) e^{[\chi(\theta-\Delta\theta)-\chi(\theta)]/\gamma}$ . In the appendix we show that, when evaluated on steering solutions, this is 1 everywhere.

Related arguments for discreteness from analyticity have been made in channel capacity problems [7–9], and there are some results about the number of points in the support of the solution [10, 11]. The maximisation problem here is more complicated, and is most similar to that of [12].

## Navigation in three dimensions

The tumble and reverse strategies have obvious generalisations to three dimensions, and figure 4A shows their performance. At low information rates reverse is again faster, with  $v/v_0 \approx \sqrt{i/6D_r}$ , and again becomes slower than tumbling at high information rates, now  $v/v_0 < 1/2$ .

Steering is more complicated, as the direction in which the agent turns is now a vector, tangent to the sphere of possible headings. The equivalent of making use of the sign of  $\theta$  is now steering always towards the pole,  $\theta = 0$ . If this is possible, then the cost of controlling  $\theta$  alone is low, producing high performance: the red points on figure 4A. However, the agent can also roll around its heading direction, which is described by an additional angle  $\psi$ . The equivalent of not knowing the sign of  $\theta$  in two-dimensional steering is not knowing this roll angle, and this greatly degrades the value of steering. If we assume the roll angle suffers from diffusion with noise  $D_\psi$ , and take  $D_\psi = D_r$  then what we see numerically is

$$v/v_0 \approx i/8D_r, \quad i \ll D_r.$$

Analytically, we can show that  $v \sim i^s$  with slope  $s \geq 1$ . This is a much steeper decline at low information rate than the discrete strategies.

The flick strategy, making right-angle turns, performs much like tumble. One difference from two dimensions is that it now has limit  $v/v_0 \rightarrow 1$  at high information rates,

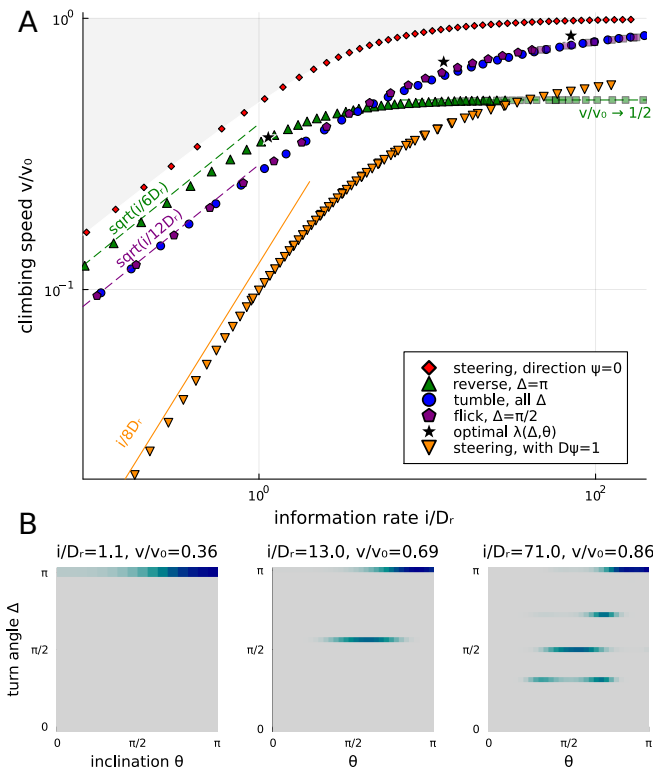


**Figure 4:** Navigation in three dimensions. (A) Performance of tumble and reverse are qualitatively similar to figure 1, with different prefactors in the  $v \propto \sqrt{i}$  scaling at low information rates. Flick produces similar performance to tumble. The red steering points are a strategy which knows which way to turn. The orange points are now a steering strategy which does not know which way to turn: the agent suffers diffusion  $D_\psi$  in its roll angle  $\psi$  (in addition to diffusion of its heading,  $D_r$ ), and this is much worse, with  $v \propto i$  at low information rates. (B) Optimal  $\lambda(\Delta, \theta)$  for a strategy allowed any turn angle  $\Delta$ . Like figure 3 we see a progression from reverse, to reverse & flick, to something more complicated.

because a succession of right-angle turns in three dimensions can bring the heading arbitrarily close to the pole. Here too we assume the roll angle is not controlled, hence each turn by  $\Delta = \pi/2$  places the heading new anywhere on a circle perpendicular to the original heading.

We can similarly study the general case where  $\lambda(\Delta, \theta)$  is the rate at which turns are initiated, placing the new heading somewhere on a circle angle  $\Delta$  away from the old heading. Figure 4B shows what we see. At low information rates, all weight is on  $\Delta = \pi$ , the reverse strategy. With more information, turns of  $\Delta \approx \pi/2$  appear too, and there are further bifurcations to use additional angles. But the distribution of turn angles remains discrete, much like in two dimensions (figure 3).

## Conclusion

In this navigation problem we see two kinds of discreteness emerge. First, among the strategies not using directional information, sudden actions like tumble and re-

verse perform better than smooth steering (figures 1, 4A). Second, if arbitrary turn angles are allowed, the optimal strategy uses a discrete set of angles (figures 3, 4B). This has parallels to the idea of rational inattention [12, 13], as well as earlier work in neural coding [14–17] and elsewhere in biology [18, 19].

While our navigation model is far too simple to quantitatively match data from any real organism, we can ask whether its qualitative features show up in the wild. Certainly many micro-organisms use strategies which alternate straight runs with sudden turns [20–22]. The transition from reverse to tumble being optimal (figures 1, 4A) could map to different bacteria which have evolved in different circumstances. For example, *V. cholerae* performs a run-reverse-flick strategy [3] when swimming fast, but only run-reverse when slow [23]. Intriguingly, the worm *C. elegans* uses a strategy qualitatively similar to our unsigned steering when certain interneurons associated with navigation are disrupted [24]. For our second kind of discreteness, evidence suggests that flies adopt discrete turn “saccades” with stereotyped angles [25], and it would be interesting to explore how this phenomenon varies with the noise level.

For our stated problem, the optimal solution is to steer in the direction of  $\theta = 0$ , the red line in Figure 1. This could be interpreted as evidence for the high value of directional information, which is even greater in three dimensions. But it’s not entirely clear that we should directly compare the information rate of such steering strategies to the others. If a limited information rate is a proxy for sensor noise, then it is difficult to imagine a sensor giving directional and undirected information with equal ease. For instance with a bilateral pair of sensors, the difference will be a noisy directional measure, while the sum will be less-noisy but non-directional. The phase diagram of strategies in this instance is unknown.

It is a limitation of our model that we do not consider time-dependent or memory-based strategies, which are used by many real microorganisms. At the simplest level, bacteria don’t measure  $\theta$ , but get a signal proportional to  $\cos \theta$  from the derivative of attractant concentration along their path. This involves storing knowledge about the past for a time of order  $1/D_r$  [6, 26, 27]. Similarly, real bacteria which using run-reverse strategy know whether their motion is forward or backward, since these directions correspond to clockwise/counter-clockwise flagellar rotation [28]. Many microorganisms swim in spirals in three dimensions [29]; this strategy could, using memory, gather information about spatial variations perpendicular to their track. In some situations *C. elegans* performs a “weathervane” motion [30], which could similarly leverage memory to measure spatial gradients. We will explore strategies which rely on memory in future work.

Finally, the mean speed up the gradient,  $v/v_0$ , isn’t the only relevant objective. If what’s being sensed is some localised food source, then there will be scenarios where the ability to loiter near to a point is also important [26], and scenarios where all that matters is being the first to ar-

rive. For travelling groups of chemotactic bacteria [31], other objectives may be important for ensuring collective navigation. Perhaps these objectives are amenable to similar study.

## Acknowledgements

We thank Marianne Bauer, Kevin Chen, Isabella Graf for comments on the draft, and Vijay Balasubramanian, Derek Sherry, Sekhar Tatikonda, Nick Weaver for discussions.

This work was supported in part by the Yale Program in Physical and Engineering Biology (J.M.B.), Mossman and NSERC Postdoctoral Fellowships (M.P.L.), and a Sloane Foundation *Matter to Life* grant (B.B.M., M.C.A.).

## References

- [1] H. C. Berg, *How bacteria swim*, *Sci. Am.* **233** (1975) 36–44.
- [2] B. L. Taylor and D. E. Koshland, *Reversal of flagellar rotation in monotrichous and peritrichous bacteria: generation of changes in direction*, *J Bacteriol* **119** (1974) 640–642.
- [3] L. Xie, T. Altindal, S. Chattopadhyay and X.-L. Wu, *Bacterial flagellum as a propeller and as a rudder for efficient chemotaxis*, *PNAS* **108** (2011) 2246–2251.
- [4] H. H. Mattingly, K. Kamino, B. B. Machta and T. Emonet, *Escherichia coli chemotaxis is information limited*, *Nat. Phys.* **17** (2021) 1426–1431 [arXiv:2102.11732].
- [5] A. J. Waite, N. W. Frankel, Y. S. Dufour, J. F. Johnston, J. Long and T. Emonet, *Non-genetic diversity modulates population performance*, *Molecular Systems Biology* **12** (2016) 895.
- [6] S. P. Strong, B. Freedman, W. Bialek and R. Koberle, *Adaptation and optimal chemotactic strategy for E. coli*, *Phys. Rev. E* **57** (1998) 4604–4617.
- [7] J. G. Smith, *The information capacity of amplitude- and variance-constrained scalar Gaussian channels*, *Information and Control* **18** (1971) 203–219.
- [8] C. Hillar and S. Marzen, *Neural network coding of natural images with applications to pure mathematics*, in *Contemporary Mathematics* (H. Harrington, M. Omar and M. Wright, eds.), vol. 685, pp. 189–221. American Mathematical Society, Providence, Rhode Island, 2017.
- [9] H. H. Mattingly, M. K. Transtrum, M. C. Abbott and B. B. Machta, *Maximizing the information learned from finite data selects a simple model*, *PNAS* **115** (2018) 1760–1765.
- [10] M. C. Abbott and B. B. Machta, *A scaling law from discrete to continuous solutions of channel capacity problems in the low-noise limit*, *J. Stat. Phys.* **176** (2019) 214–227.
- [11] L. Barletta, A. Dytso and S. Shamai, *Improved bounds on the number of support points of the capacity-achieving input for amplitude constrained Poisson channels*, arXiv:2401.05045.
- [12] J. Jung, J. H. J. Kim, F. Matějka and C. A. Sims, *Discrete actions in information-constrained decision problems*, *Rev. Econ. Stud.* **86** (2019) 2643–2667.
- [13] C. A. Sims, *Rational inattention: Beyond the linear-quadratic case*, *Am. Econ. Rev.* **96** (2006) 158–163.
- [14] A. P. Nikitin, N. G. Stocks, R. P. Morse and M. D. McDonnell, *Neural population coding is optimized by discrete tuning curves*, *Phys. Rev. Lett.* **103** (2009) 138101.
- [15] D. B. Kastner, S. A. Baccus and T. O. Sharpee, *Critical and maximally informative encoding between neural populations in the retina*, *PNAS* **112** (2015) 2533–2538.
- [16] T. O. Sharpee, *Optimizing neural information capacity through discretization*, *Neuron* **94** (2017) 954–960.
- [17] S. Shao, M. Meister and J. Gjorgjieva, *Efficient population coding of sensory stimuli*, *Phys. Rev. Research* **5** (2023) 043205.
- [18] G. Tkacik, C. G. Callan and W. Bialek, *Information flow and optimization in transcriptional regulation*, *PNAS* **105** (2008) 12265–12270 [arXiv:0705.0313].
- [19] O. Witteveen, S. J. Rosen, R. S. Lach, M. Z. Wilson and M. Bauer, *Optimizing information transmission in optogenetic Wnt signaling*, *Phys Rev Res.* (2026) [arXiv:2506.22633].
- [20] M. Grognot and K. M. Taute, *More than propellers: how flagella shape bacterial motility behaviors*, *Current Opinion in Microbiology* **61** (2021) 73–81.
- [21] M. Grognot, A. Mittal, M. Mah’moud and K. M. Taute, *Vibrio cholerae motility in aquatic and mucus-mimicking environments*, *Appl. Environ. Microbiol.* **87** (2021) e01293–21.
- [22] M. Grognot, J. W. Nam, L. E. Elson and K. M. Taute, *Physiological adaptation in flagellar architecture improves Vibrio alginolyticus chemotaxis in complex environments*, *PNAS* **120** (2023) e2301873120.
- [23] K. Son, F. Menolascina and R. Stocker, *Speed-dependent chemotactic precision in marine bacteria*, *PNAS* **113** (2016) 8624–8629.
- [24] K. S. Chen, A. K. Sharma, J. W. Pillow and A. M. Leifer, *Navigation strategies in Caenorhabditis elegans are differentially altered by learning*, *PLoS Biol* **23** (2025) e3003005.
- [25] M. Demir, N. Kadakia, H. D. Anderson, D. A. Clark and T. Emonet, *Walking Drosophila navigate complex plumes using stochastic decisions biased by the timing of odor encounters*, *eLife* **9** (2020).
- [26] D. A. Clark and L. C. Grant, *The bacterial chemotactic response reflects a compromise between transient and steady-state behavior*, *PNAS* **102** (2005) 9150–9155.
- [27] A. Celani and M. Vergassola, *Bacterial strategies for chemotaxis response*, *PNAS* **107** (2010) 1391–1396.
- [28] K. Son, J. S. Guasto and R. Stocker, *Bacteria can exploit a flagellar buckling instability to change direction*, *Nature physics* **9** (2013), no. 8 494–498.
- [29] A. Battista, F. Frischknecht and U. S. Schwarz, *Geometrical model for malaria parasite migration in structured environments*, *Phys. Rev. E* **90** (2014) 042720.
- [30] Y. Iino and K. Yoshida, *Parallel use of two behavioral mechanisms for chemotaxis in Caenorhabditis elegans*, *J. Neurosci.* **29** (2009) 5370–5380.
- [31] L. Vo, F. Avgidis, H. H. Mattingly, K. Edmonds, I. Burger, R. Balasubramanian, T. S. Shimizu, B. I. Kazmierczak and T. Emonet, *Nongenetic adaptation by collective migration*, *PNAS* **122** (2025) e2423774122.
- [32] G. B. Arfken and H. J. Weber, *Mathematical methods for physicists 6th ed.* Elsevier, 2005.

- [33] Z. Hradil, J. Řeháček, Z. Bouchal, R. Čelechovský and LL. Sánchez-Soto, *Minimum uncertainty measurements of angle and angular momentum*, *Phys. Rev. Lett.* **97** (2006) 243601 [[arXiv:quant-ph/0605137](#)].
- [34] J. Řeháček, Z. Bouchal, R. Čelechovský, Z. Hradil and LL. Sánchez-Soto, *Experimental test of uncertainty relations for quantum mechanics on a circle*, *Phys. Rev. A* **77** (2008) 032110 [[arXiv:0712.0230](#)].

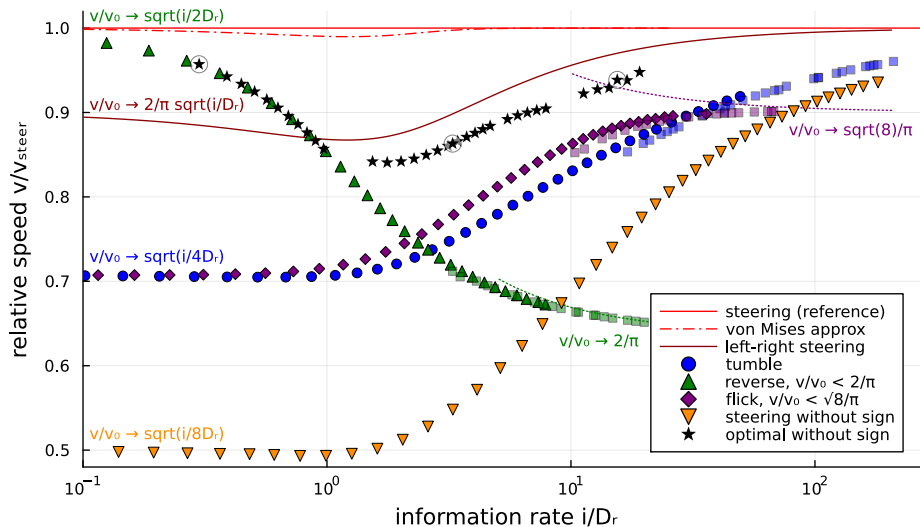


**Figure S1:** Performance of strategies for two-dimensional navigation, relative to steering. Shows most of the data in figure 1, but adds a lines for the exact left-right steering solution (dark red, section C 5), and numerical points for the flick solution (purple) and the optimal symmetric  $\lambda(\Delta\theta|\theta)$  (black stars). If we ignore the black stars, then notice that three different unsigned solutions are optimal in turn – reverse at low information rate, then flick, then tumble. As before, square plot points indicate the use of the ansatz  $\lambda_{\text{strong}}(\theta)$ , while others solve for the whole function.

## Appendix A. Additional figures

Figure 1 in the main text compares the performance of four strategies, and observes that steering (the red line) is fastest. Figure S1 shows the same data plotted relative to the steering solution, and adds several more strategies.

Figures S2 and S3 show some more numerical trajectories, first with the same parameters as figure 2E in the main text (all  $i/D_r \approx 0.1$ ), and then with much higher information rates ( $i/D_r \approx 5$ ). Observe particularly the steering solutions without the sign (rightmost panels) which make progress diagonally, and make occasional full turns. We make a sign choice in plotting these, as there is always an equivalent strategy,  $-\mu(\theta)$ , which goes diagonally the other way.

## Appendix B. Analytic results for factorised discrete strategies

Here we derive some results for solutions whose jump rate is of the form  $\lambda(\Delta\theta, \theta) = \lambda(\theta)q(\Delta\theta)$ , where  $q$  is a probability distribution over target angles. We also assume that the target distribution is symmetric, such that  $q(\Delta\theta) = q(-\Delta\theta)$ . The tumble, reverse, and flick strategies are in this class.

At low information rates, we study small deviations from constant  $\lambda(\theta)$ , and are able to derive the  $v \propto \sqrt{i}$  scaling law. We then show how to introduce a finite time-penalty per discrete action, and derive the effect on the  $v \propto \sqrt{i}$  law. Finally, in Section B 3 we make an ansatz for steady-state  $p(\theta)$  to be a von Mises distribution, which works well for the reverse strategy.

For this class of strategies, the Fokker-Planck equation reads

$$\frac{dp(\theta)}{dt} = -\lambda(\theta)p(\theta) + \int d\Delta\theta \lambda(\theta - \Delta\theta)p(\theta - \Delta\theta)q(\Delta\theta) + D_r p''(\theta), \quad (\text{B1})$$

and the information rate is the same as (3)

$$i = \int d\theta p(\theta) \lambda(\theta) \log \left( \frac{\lambda(\theta)}{\langle \lambda \rangle} \right), \quad (\text{B2})$$

where  $\langle \lambda \rangle = \langle \lambda(\theta) \rangle_\theta = \int d\theta p(\theta) \lambda(\theta)$ .

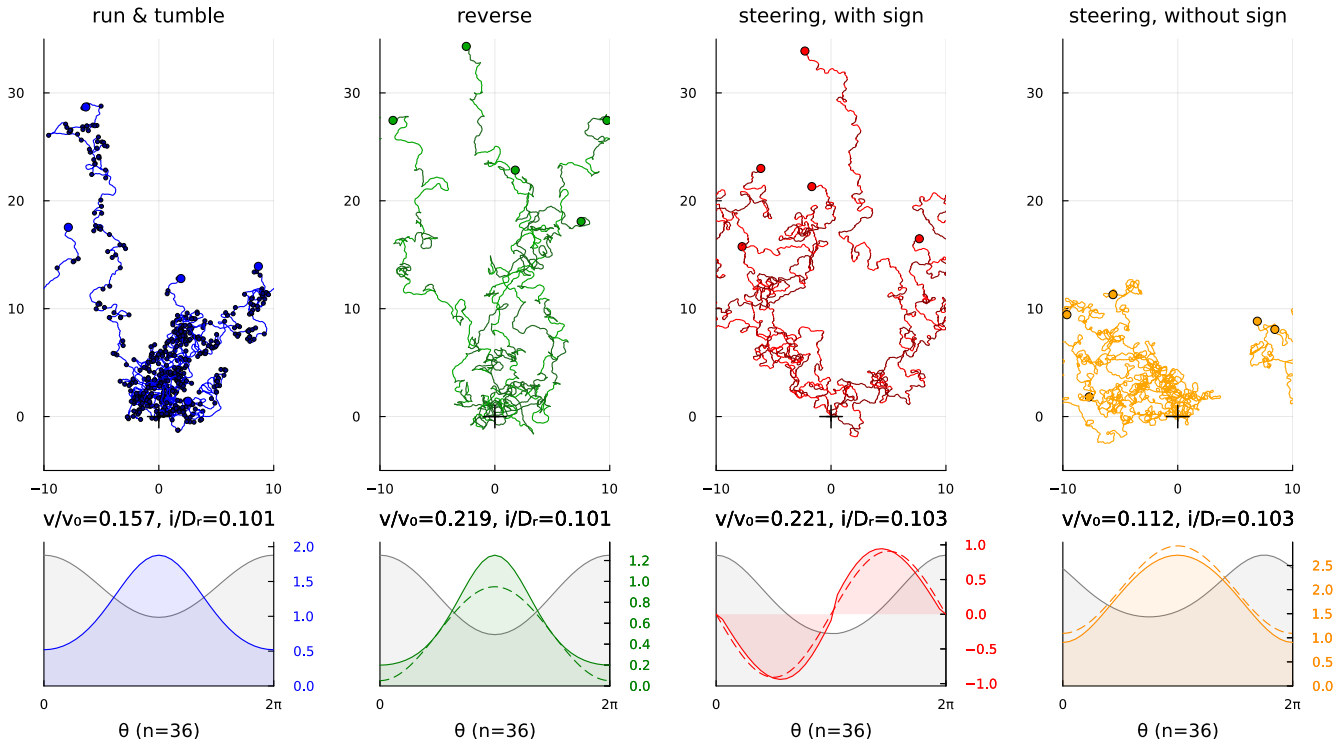


**Figure S2:** Sample trajectories for four strategies, all with the same information rate  $i/D_r \approx 0.1$ . Similar to as figure 2E, except showing five examples of each strategy. Each reversal changes the line colour between dark and light green. Steering changes between light and dark red according to the sign of  $\mu(\theta)$ . At low information rates, unsigned steering has  $\langle \cos \theta \rangle_\theta \approx \pm \langle \sin \theta \rangle_\theta$ , so the agent goes sideways as much as up the gradient. All plots are for time  $0 < t < 100$ , and wrapped to  $-10 < x < 10$ , in units  $D_r = v_0 = 1$ .

### B.1 Solution at low information rate

At low information rate, we use a perturbative ansatz. We posit that there is some parameter  $\epsilon$ , which vanishes as  $\gamma \rightarrow \infty$ , such that our strategy can be written as

$$\lambda(\theta) = \lambda_c(1 + \epsilon\lambda^{(1)}(\theta) + \epsilon^2\lambda^{(2)}(\theta) + \dots), \quad (\text{B3})$$

where the only dependency on  $\gamma$  is through  $\epsilon$  and potentially  $\lambda_c$ . Since we have the freedom to choose  $\lambda_c$  and  $\epsilon$  to set the scale, we can choose our first-order perturbation to satisfy

$$\int d\theta \lambda^{(1)}(\theta) = 0, \quad \frac{1}{2\pi} \int d\theta \lambda^{(1)}(\theta)^2 = 1. \quad (\text{B4})$$

Intuitively, we allow for a non-zero rate as  $\epsilon \rightarrow 0$  since all constant strategies use no information, but also have zero drift velocity. The second constraint ensures that the scale of the perturbation is fixed by  $\epsilon$ .

We also expand the stationary density in  $\epsilon$ :

$$p(\theta) = \frac{1}{2\pi}(1 + \epsilon p^{(1)}(\theta) + \epsilon^2 p^{(2)}(\theta) + \dots). \quad (\text{B5})$$

Due to normalization, we must have

$$\int d\theta p^{(k)}(\theta) = 0. \quad (\text{B6})$$

Under these choices, the rest of the structure of the solution should arise from optimality. We allow the distribution  $q(\Delta\theta)$  to be arbitrary, as long as it is symmetric.

Using our ansatz in the master equation and collecting the first-order terms in  $\epsilon$ , we obtain

$$0 = \frac{D_r}{2\pi} \partial_\theta^2 p^{(1)}(\theta) - \frac{\lambda_c}{2\pi} [p^{(1)}(\theta) + \lambda^{(1)}(\theta)] + \frac{\lambda_c}{(2\pi)^2} \int d\theta' [p^{(1)}(\theta') + \lambda^{(1)}(\theta')] q(\theta - \theta'). \quad (\text{B7})$$

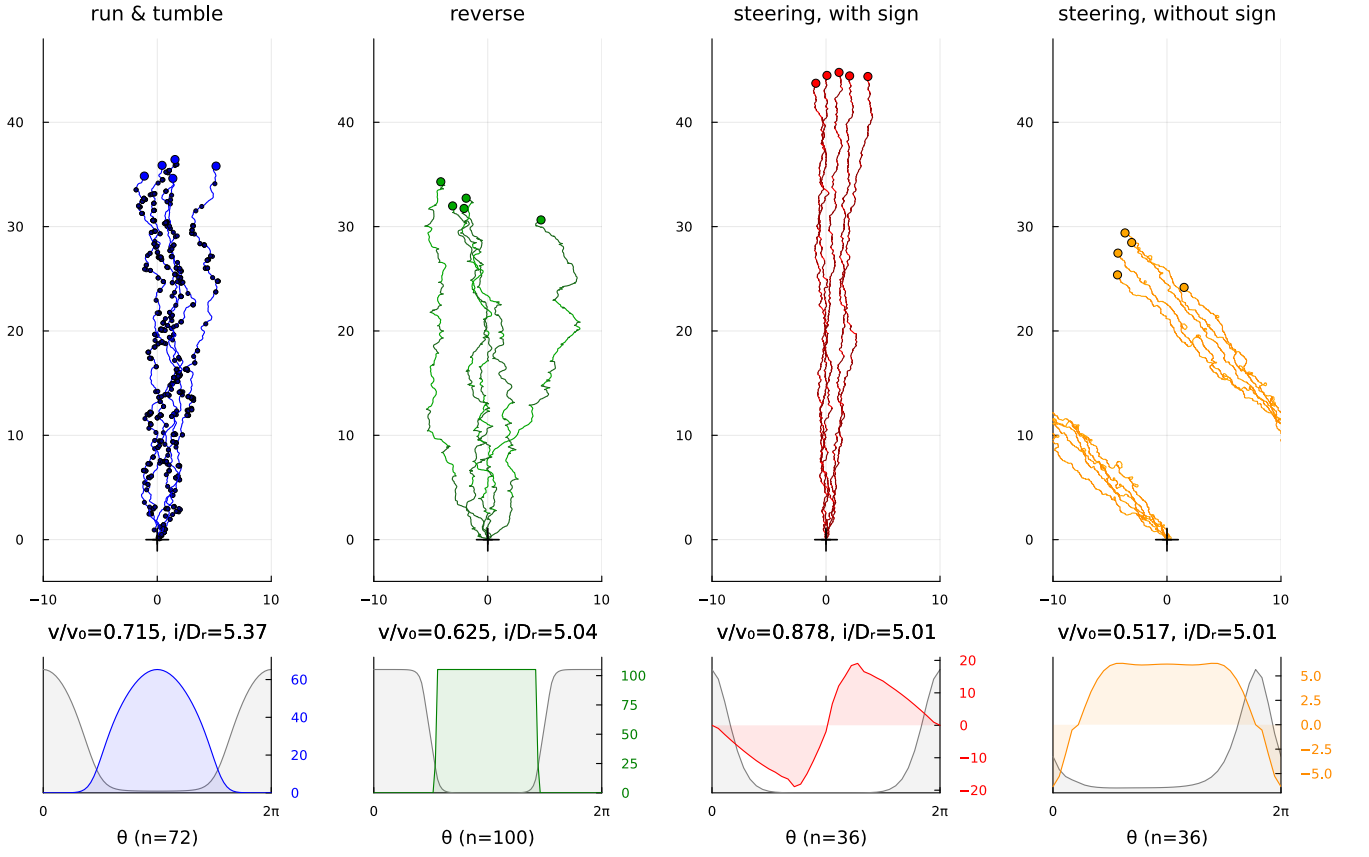


**Figure S3:** Sample trajectories for four strategies, with a higher information rate  $i/D_r \approx 5$ . All plots for time  $0 < t < 50$ . Compared to figure S2, these are half the duration, with 50x the information rate.

We now transform this equation to obtain its Fourier coefficients, using the following convention:

$$g_n = \frac{1}{2\pi} \int d\theta e^{-in\theta} g(\theta). \quad (\text{B8})$$

With this, the Fourier modes of our first-order corrections satisfy

$$0 = -D_r n^2 p_n^{(1)} - \lambda_c [p_n^{(1)} + \lambda_n^{(1)}] + 2\pi \lambda_c [p_n^{(1)} + \lambda_n^{(1)}] q_n. \quad (\text{B9})$$

Solving for  $p_n^{(1)}$  we obtain

$$p_n^{(1)} = - \left( \frac{\lambda_c [1 - 2\pi q_n]/D_r}{n^2 + \lambda_c [1 - 2\pi q_n]/D_r} \right) \lambda_n^{(1)}. \quad (\text{B10})$$

Therefore, our drift velocity can be written explicitly in terms of our strategy  $(\lambda, q)$ :

$$\langle \cos(\theta) \rangle_\theta = \epsilon \frac{p_1^{(1)} + p_{-1}^{(1)}}{2} + \mathcal{O}(\epsilon^2) = -\frac{\epsilon}{2} \left( \frac{\lambda_c [1 - 2\pi q_n]/D_r}{1 + \lambda_c [1 - 2\pi q_n]/D_r} \right) [\lambda_1^{(1)} - \lambda_{-1}^{(1)}] + \mathcal{O}(\epsilon^2), \quad (\text{B11})$$

where we used the symmetry of  $q$  to conclude that  $q_1 = q_{-1} \in \mathbb{R}$ .

Just like we can do a perturbative expansion of the drift velocity, we can do a perturbative expansion of the information rate. The leading order of this expansion will be  $\epsilon^2$ , so we want to keep all terms up to this order. First, we compute the average

$$\langle \lambda \rangle = \frac{\lambda_c}{2\pi} \int d\theta [1 + \epsilon p^{(1)}(\theta) + \epsilon^2 p^{(2)}(\theta) + \dots] [1 + \epsilon \lambda^{(1)}(\theta) + \epsilon^2 \lambda^{(2)}(\theta) + \dots]. \quad (\text{B12})$$

We obtain

$$\langle \lambda \rangle = \lambda_c \left[ 1 + \epsilon^2 \lambda_0^{(2)} + \epsilon^2 \frac{1}{2\pi} \int d\theta p^{(1)}(\theta) \lambda^{(1)}(\theta) + \mathcal{O}(\epsilon^3) \right]. \quad (\text{B13})$$

Doing a perturbative expansion of the logarithm, this implies that

$$\log \left( \frac{\lambda_c}{\langle \lambda \rangle} \right) = -\epsilon^2 \lambda_0^{(2)} - \epsilon^2 \frac{1}{2\pi} \int d\theta p^{(1)}(\theta) \lambda^{(1)}(\theta) + \mathcal{O}(\epsilon^3). \quad (\text{B14})$$

Similarly, we have that

$$\log \left( \frac{\lambda(\theta)}{\lambda_c} \right) = \epsilon \lambda^{(1)}(\theta) + \epsilon^2 \lambda^{(2)}(\theta) - \frac{\epsilon^2}{2} \lambda^{(1)}(\theta)^2 + \mathcal{O}(\epsilon^3). \quad (\text{B15})$$

Grouping terms together, we obtain

$$\log \left( \frac{\lambda(\theta)}{\langle \lambda \rangle} \right) = \epsilon \lambda^{(1)}(\theta) + \epsilon^2 \left[ \lambda^{(2)}(\theta) - \lambda_0^{(2)} - \frac{1}{2} \lambda^{(1)}(\theta)^2 - \frac{1}{2\pi} \int d\theta' p^{(1)}(\theta') \lambda^{(1)}(\theta') \right] + \mathcal{O}(\epsilon^3). \quad (\text{B16})$$

The expansion for  $p(\theta)\lambda(\theta)$  is

$$p(\theta)\lambda(\theta) = \frac{\lambda_c}{2\pi} \left[ 1 + \epsilon(p^{(1)}(\theta) + \lambda^{(1)}(\theta)) + \mathcal{O}(\epsilon^2) \right]. \quad (\text{B17})$$

These two expansions are sufficient to obtain all the terms to order  $\epsilon^2$ .

Let us now decompose the information rate into two terms:  $i = i_1 + i_2 + \mathcal{O}(\epsilon^3)$ , given by

$$\begin{aligned} i_1 &= \epsilon^2 \frac{\lambda_c}{2\pi} \int d\theta [p^{(1)}(\theta) + \lambda^{(1)}(\theta)] \lambda^{(1)}(\theta), \\ i_2 &= \epsilon^2 \frac{\lambda_c}{2\pi} \int d\theta \left[ \lambda^{(2)}(\theta) - \lambda_0^{(2)} - \frac{1}{2} \lambda^{(1)}(\theta)^2 - \frac{1}{2\pi} \int d\theta' p^{(1)}(\theta') \lambda^{(1)}(\theta') \right]. \end{aligned} \quad (\text{B18})$$

In  $i_2$ , we can easily see that the first two terms cancel, so we obtain

$$i_2 = -\epsilon^2 \frac{\lambda_c}{2\pi} \int d\theta \left[ p^{(1)}(\theta) \lambda^{(1)}(\theta) + \frac{1}{2} \lambda^{(1)}(\theta)^2 \right]. \quad (\text{B19})$$

Bringing these terms together, we obtain the leading-order term for the information rate:

$$i = \frac{\epsilon^2 \lambda_c}{4\pi} \int d\theta \lambda^{(1)}(\theta)^2 + \mathcal{O}(\epsilon^3) = \frac{1}{2} \epsilon^2 \lambda_c + \mathcal{O}(\epsilon^3), \quad (\text{B20})$$

where the last equality comes from the choice of scale we made in our expansion.

We can now state the optimization problem for the leading-order terms in drift velocity and information rate:

$$\max_{\lambda^{(1)}, \lambda_c, \epsilon} \left\{ \underbrace{-\frac{\epsilon}{2} \left( \frac{\lambda_c [1 - 2\pi q_1] / D_r}{1 + \lambda_c [1 - 2\pi q_1] / D_r} \right)}_{v/v_0} [\lambda_1^{(1)} + \lambda_{-1}^{(1)}] - \underbrace{\gamma \frac{1}{2} \epsilon^2 \lambda_c}_i \right\}. \quad (\text{B21})$$

Note that we allow  $\epsilon$  to be chosen optimally. Our solution is consistent if the optimal epsilon vanishes as  $\gamma \rightarrow \infty$ . Additionally, we keep our  $q$  strategy fixed for now. First, note that the information rate does not depend on the structure of the  $\lambda^{(1)}$  modes. Therefore, it is optimal to just keep the  $n = \pm 1$  modes and choose them to be  $-1/\sqrt{2}$ , such that  $\lambda^1(\theta) = -\sqrt{2} \cos(\theta)$ . The optimization problem, then, becomes

$$\max_{\lambda_c, \epsilon} \left\{ \frac{\epsilon}{\sqrt{2}} \left( \frac{\lambda_c [1 - 2\pi q_1] / D_r}{1 + \lambda_c [1 - 2\pi q_1] / D_r} \right) - \gamma \frac{1}{2} \epsilon^2 \lambda_c \right\}. \quad (\text{B22})$$

Solving for the optimal  $\epsilon$  and  $\lambda_c$  yields

$$\begin{aligned} \epsilon^* &= \frac{1 - 2\pi q_1}{2\sqrt{2}\gamma D_r}, \\ \lambda_c^* &= \frac{D_r}{1 - 2\pi q_1}. \end{aligned} \quad (\text{B23})$$

This justifies our initial choice of the perturbative ansatz, since  $\epsilon^*$  scales as  $1/\gamma$  and  $\lambda_c^*$  is independent of  $\gamma$ .

Under the optimal strategy, we can find a relationship between the drift velocity and the information rate, which yields our low-information Pareto frontier:

$$\frac{v}{v_0} = \left( \frac{i[1 - 2\pi q_1]}{4D_r} \right)^{1/2}. \quad (\text{B24})$$

We can see what this frontier is for some of the strategies we analyze in the main text. For run and tumble, we have  $q(\Delta\theta) = 1/2\pi$ , so  $q_1 = 0$ . Therefore, its Pareto frontier scales as

$$\left( \frac{v}{v_0} \right)_{\text{tumbles}} = \left( \frac{i}{4D_r} \right)^{1/2}. \quad (\text{B25})$$

The target distribution for the reversing strategy is  $q(\Delta\theta) = \delta(\Delta\theta - \pi)$ . This means  $q_1 = -1/2\pi$ , so the Pareto frontier is

$$\left( \frac{v}{v_0} \right)_{\text{reverse}} = \left( \frac{i}{2D_r} \right)^{1/2}. \quad (\text{B26})$$

In fact, reversing achieves the highest possible drift velocity in this regime. For any symmetric strategy  $q$ , we have that

$$q_1 = \frac{1}{2\pi} \int_0^{2\pi} d\Delta\theta e^{-i\Delta\theta} q(\theta) = \frac{1}{2\pi} \int_0^{2\pi} d\Delta\theta \cos(\Delta\theta) q(\theta) = \frac{1}{2\pi} \langle \cos(\Delta\theta) \rangle_q. \quad (\text{B27})$$

Since  $\cos(\Delta\theta) \geq -1$ , we must have

$$q_1 \geq -\frac{1}{2\pi}. \quad (\text{B28})$$

Since the reversing strategy saturates this bound, and the scaling of the frontier only depends on  $q_1$ , we conclude that it is the optimal low-information strategy.

In addition to the information rate, we can find the leading-order behavior of the jump rate. In terms of  $\lambda^*$  and  $\epsilon^*$ , this is

$$\lambda(\theta) \approx \lambda_c^* \left[ 1 - \sqrt{2}\epsilon^* \cos(\theta) \right]. \quad (\text{B29})$$

Using our solution and writing these in terms of  $i$ , we obtain

$$\lambda(\theta) \approx \frac{D_r}{1 - 2\pi q_1} \left[ 1 - 2 \left( \frac{i}{D_r} \right)^{1/2} (1 - 2\pi q_1)^{1/2} \cos(\theta) \right]. \quad (\text{B30})$$

## B.2 Time penalty for tumbles or other actions

So far we have considered instantaneous changes of heading, but any real organisms takes a finite amount of time to turn. For example, tumbles take up order 10% of an *E. coli*'s time. To build this into our framework, we now introduce a time penalty  $\tau$  for each tumble, or other action. We write  $\bar{p}_\tau(t)$  for the proportion of time spent tumbling, and  $\bar{p}(\theta, t)$  for the rest of the time. These obey

$$\bar{p}_\tau(t) = \int_{t-\tau}^t dt' \int d\theta \lambda(\theta) \bar{p}(\theta, t-t'), \quad \bar{p}_\tau(t) + \int d\theta \bar{p}(\theta, t) = 1. \quad (\text{B31})$$

The Fokker-Planck equation for  $d\bar{p}(\theta, t)/dt$  takes the same form as above, except that it needs a time delay in the source term:  $\int d\Delta\theta \lambda(\theta - \Delta\theta) \bar{p}(\theta - \Delta\theta, t - \tau) q(\Delta\theta)$ . This linear equation has steady-state solution  $\bar{p}(\theta, t) = \eta p(\theta)$ , where  $p(\theta)$  is the normalized density solving the original ( $\tau = 0$ ) equation above. Solving, we get

$$\bar{p}_\tau(t) = 1 - \eta, \quad \eta = \frac{1}{1 + \tau \langle \lambda(\theta) \rangle_\theta}, \quad (\text{B32})$$

where the expectation value is still with respect to  $p(\theta)$ , i.e.  $\langle \lambda(\theta) \rangle_\theta = \int d\theta p(\theta) \lambda(\theta)$ . The up-gradient relative speed averages over only the time not spent tumbling:

$$v/v_0 = \int d\theta \bar{p}(\theta, t) \cos \theta = \eta \langle \cos \theta \rangle_\theta. \quad (\text{B33})$$

Therefore, our optimization problem now reads:

$$\max_{\lambda, q} \frac{\langle \cos \theta \rangle_\theta}{1 + \tau \langle \lambda(\theta) \rangle_\theta} - \gamma i. \quad (\text{B34})$$

In the low information regime, we can use the perturbative expansions in the previous section. From Eq. (B13), we have that the corrections to  $\langle \lambda \rangle$  are of second order in  $\epsilon$ . Therefore, following the procedure in the previous section, we arrive at the leading-order optimization problem for a fixed  $q$ :

$$\max_{\lambda_c, \epsilon} \left\{ \frac{\epsilon}{\sqrt{2}(1 + \tau \lambda_c)} \left( \frac{\lambda_c [1 - 2\pi q_1]/D_r}{1 + \lambda_c [1 - 2\pi q_1]/D_r} \right) - \gamma \frac{1}{2} \epsilon^2 \lambda_c \right\}. \quad (\text{B35})$$

Recall that  $q_1$  is the first Fourier mode of  $q(\Delta\theta)$ . Solving the problem gives the frontier

$$\frac{v}{v_0} = \left( \frac{i[1 - 2\pi q_1]}{4D_r} \right)^{1/2} U \left( \frac{D_r \tau}{1 - 2\pi q_1} \right), \quad (\text{B36})$$

where  $U$  is a universal function given by

$$U(x) := \frac{2\sqrt{\phi(x)}}{(1 + x\phi(x))(1 + \phi(x))}, \quad \phi(x) := \frac{-(1 + x) + \sqrt{(1 + x)^2 + 12x}}{6x}. \quad (\text{B37})$$

Importantly,  $U$  is decreasing and satisfies  $U(0) = 1$  and  $U(x \rightarrow \infty) \rightarrow 0$ . For intuition, it is useful to note that  $U$  satisfies

$$\left( \frac{1}{2 + x} \right)^{1/2} \leq U(x) \leq \left( \frac{1}{1 + x} \right)^{1/2}. \quad (\text{B38})$$

We can evaluate the value of the time delay  $\tau$  for which tumbling and reversing perform worse than unsigned steering at low information. For tumbles  $q_1 = 0$ , so the critical  $\tau$  is determined by

$$U(D_r \tau_{\text{tumbles}}) = \frac{1}{\sqrt{2}} \implies D_r \tau_{\text{tumbles}} \approx 0.694. \quad (\text{B39})$$

For reversing, we have  $q_1 = -1/2\pi$ . Therefore, the critical  $\tau$  is determined by

$$U \left( \frac{D_r \tau_{\text{reverse}}}{2} \right) = \frac{1}{2} \implies D_r \tau_{\text{reverse}} \approx 4.907. \quad (\text{B40})$$

### B.3 Parametric ansatz for reverse strategies

For a given strategy, we can parametrize a form of the stationary distribution that seems consistent with the numerical solutions. In particular, we will characterize the distributions in terms of a width parameter  $\kappa$ , and denote them with  $p_\kappa(\theta)$ . Our optimization problem, then, is

$$\max_{\kappa, \lambda} \{ \langle \cos(\theta) \rangle_\theta - \gamma i \}, \quad (\text{B41})$$

subject to the condition that  $\lambda$  generates  $p_\kappa$  as the stationary distribution. Conditional on  $\kappa$ , the drift velocity  $\langle \cos(\theta) \rangle_\theta$  is only determined by  $p_\kappa$ . Therefore, we can solve the optimization process in two steps. First, define

$$\lambda_\kappa := \underset{\lambda}{\operatorname{argmin}} i. \quad (\text{B42})$$

That is, first we solve for the jump rate that minimizes the information rate subject to the master-equation constraint. Then we can perform the maximization over  $\kappa$  for a given  $\gamma$ . However, if the problem is sufficiently nice, we only need to solve the problem (min  $\lambda$ ) and the Pareto frontier will be traced out by varying  $\kappa$ .

The stationarity condition for reversing takes the form

$$D_r p''(\theta) - p(\theta)\lambda(\theta) + p(\theta + \pi)\lambda(\theta + \pi) = 0. \quad (\text{B43})$$

This gives an interesting constraint on our stationary distribution:

$$p''(\theta) = -p''(\theta + \pi). \quad (\text{B44})$$

Knowing this, and looking at the numerical results, we propose the following ansatz for the stationary distribution:

$$p_\kappa(\theta) = \frac{1}{\pi} \Phi(\kappa \cos(\theta)), \quad (\text{B45})$$

where  $\Phi$  is a smooth CDF, which satisfies  $\Phi(-x) = 1 - \Phi(x)$ . This distribution satisfies the anti-symmetry constraint and smoothly interpolates between a uniform distribution and a uniform distribution on the interval  $[-\pi/2, \pi/2]$ .

We want to optimize for the jump rate that minimizes the information rate. We can write the information rate in terms of the jump rate on the interval  $[-\pi/2, \pi/2]$ :

$$i = \int_{-\pi/2}^{\pi/2} d\theta \left[ p(\theta)\lambda(\theta) \log \left( \frac{\lambda(\theta)}{\langle \lambda \rangle} \right) + p(\theta + \pi)\lambda(\theta + \pi) \log \left( \frac{\lambda(\theta + \pi)}{\langle \lambda \rangle} \right) \right]. \quad (\text{B46})$$

This allows us to explicitly incorporate the constraint, since  $\lambda(\theta)$  and  $\lambda(\theta + \pi)$  cannot be independently varied. Using our constraint, we can write this as

$$i = \int_{-\pi/2}^{\pi/2} d\theta \left[ p(\theta)\lambda(\theta) \log \left( \frac{\lambda(\theta)}{\langle \lambda \rangle} \right) + [p(\theta)\lambda(\theta) - D_r p''(\theta)] \log \left( \frac{p(\theta)\lambda(\theta) - D_r p''(\theta)}{p(\theta + \pi)\langle \lambda \rangle} \right) \right]. \quad (\text{B47})$$

Additionally, we can write the average jumping rate as

$$\langle \lambda \rangle = \int_{-\pi/2}^{\pi/2} d\theta [p(\theta)\lambda(\theta) + p(\theta + \pi)\lambda(\theta + \pi)]. \quad (\text{B48})$$

With the constraint, this becomes

$$\langle \lambda \rangle = \int_{-\pi/2}^{\pi/2} d\theta [2p(\theta)\lambda(\theta) - D_r p''(\theta)]. \quad (\text{B49})$$

Simplifying:

$$\langle \lambda \rangle = 2 \int_{-\pi/2}^{\pi/2} d\theta p(\theta)\lambda(\theta) - D_r [p'(\pi/2) - p'(-\pi/2)]. \quad (\text{B50})$$

This gives us our first functional derivative:

$$\frac{\delta \langle \lambda \rangle}{\delta \lambda(\theta)} = 2p(\theta). \quad (\text{B51})$$

With this setup, we can write our first-order condition as

$$\frac{\delta i}{\delta \lambda(\theta)} = 0. \quad (\text{B52})$$

Taking this variation explicitly yields

$$\begin{aligned} \frac{\delta i}{\delta \lambda(\theta)} = & p(\theta) \log \left( \frac{\lambda(\theta)}{\langle \lambda \rangle} \right) + p(\theta) \log \left( \frac{p(\theta)\lambda(\theta) - D_r p''(\theta)}{p(\theta + \pi)\langle \lambda \rangle} \right) \\ & + 2p(\theta) - \int_{-\pi/2}^{\pi/2} d\theta' \left[ \frac{p(\theta')\lambda(\theta')}{\langle \lambda \rangle} + \frac{p(\theta')\lambda(\theta') - D_r p''(\theta')}{\langle \lambda \rangle} \right] \frac{\delta \langle \lambda \rangle}{\delta \lambda(\theta)}. \end{aligned} \quad (\text{B53})$$

Note that this last integral evaluates to  $2p(\theta)$ . Therefore, we can simplify the FOC to

$$\log\left(\frac{\lambda(\theta)}{\langle\lambda\rangle}\right) + \log\left(\frac{p(\theta)\lambda(\theta) - D_r p''(\theta)}{p(\theta + \pi)\langle\lambda\rangle}\right) = 0. \quad (\text{B54})$$

This implies that

$$\lambda(\theta)\lambda(\theta + \pi) = \langle\lambda\rangle^2. \quad (\text{B55})$$

Note that this result holds regardless of the parametric ansatz.

This result gets us most of the way to characterizing the solution. For a given  $\kappa$ , let  $\tilde{\lambda}_\kappa(\theta) := \lambda_\kappa(\theta)/\langle\lambda_\kappa\rangle$ . Then our optimality condition is

$$\tilde{\lambda}_\kappa(\theta)\tilde{\lambda}_\kappa(\theta + \pi) = 1. \quad (\text{B56})$$

Multiplying by  $p(\theta)p(\theta + \pi)$  and using our constraint, we obtain

$$p_\kappa(\theta)\tilde{\lambda}_\kappa(\theta) \left[ p_\kappa(\theta)\tilde{\lambda}_\kappa(\theta) - \frac{D_r}{\langle\lambda_\kappa\rangle} p_\kappa''(\theta) \right] = p_\kappa(\theta)p_\kappa(\theta + \pi). \quad (\text{B57})$$

Another nice property of our ansatz is that  $p_\kappa(\theta + \pi) = \frac{1}{\pi} - p_\kappa(\theta)$ . Therefore, we obtain

$$p_\kappa(\theta)\tilde{\lambda}_\kappa(\theta) \left[ p_\kappa(\theta)\tilde{\lambda}_\kappa(\theta) - \frac{D_r}{\langle\lambda_\kappa\rangle} p_\kappa''(\theta) \right] = p_\kappa(\theta) \left[ \frac{1}{\pi} - p_\kappa(\theta) \right]. \quad (\text{B58})$$

We can solve for  $p_\kappa(\theta)\tilde{\lambda}_\kappa(\theta)$ :

$$p_\kappa(\theta)\tilde{\lambda}_\kappa(\theta) = \frac{D_r}{2\langle\lambda_\kappa\rangle} p_\kappa''(\theta) + \left( \frac{D_r^2}{4\langle\lambda_\kappa\rangle^2} p_\kappa''(\theta)^2 + p_\kappa(\theta) \left[ \frac{1}{\pi} - p_\kappa(\theta) \right] \right)^{1/2}. \quad (\text{B59})$$

Additionally, note that by definition

$$\int d\theta p_\kappa(\theta)\tilde{\lambda}_\kappa(\theta) = 1. \quad (\text{B60})$$

Therefore,  $\langle\lambda_\kappa\rangle$  must satisfy the fixed-point equation

$$\langle\lambda_\kappa\rangle = \int d\theta \left( \frac{D_r^2}{4} p_\kappa''(\theta)^2 + p_\kappa(\theta) \left[ \frac{1}{\pi} - p_\kappa(\theta) \right] \langle\lambda_\kappa\rangle^2 \right)^{1/2}. \quad (\text{B61})$$

Once  $\langle\lambda_\kappa\rangle$  is determined, the optimal jump rate is

$$\lambda_\kappa(\theta) = \frac{1}{p_\kappa(\theta)} \left[ \frac{D_r}{2} p_\kappa''(\theta) + \left( \frac{D_r^2}{4} p_\kappa''(\theta)^2 + p_\kappa(\theta) \left[ \frac{1}{\pi} - p_\kappa(\theta) \right] \langle\lambda_\kappa\rangle^2 \right)^{1/2} \right]. \quad (\text{B62})$$

For a given  $\kappa$ , this gives us a routine to find a point on the estimated frontier, since we can evaluate the drift velocity and information rate using  $p_\kappa(\theta)$  and  $\langle\lambda_\kappa\rangle$ .

## Appendix C. Analytic results for continuous steering

Here we derive analytic results for the strategies when only continuous steering  $\mu(\theta)$  is used, with no discrete jumps. First, we derive the information rate (3); see also Section E 2 below for a derivation in  $d$  dimensions.

Then we find some optimal solutions, starting with most general version where the agent can measure the full heading  $\theta$ , which we call signed information. We also consider a variant where the agent has access only to the sign, left or right, for which we find a much simpler analytic solution. Finally, we treat the case of steering without the sign, where we have an analytic solution only at low information rates.

### C.1 Steering and diffusion as turns $\Delta\theta = \pm\alpha$

We can write the controlled update for  $\theta$  for steering and diffusion in short time  $\Delta t$  as follows:

$$\Delta\theta = \mu(\theta)\Delta t + \sqrt{2D_c\Delta t}\eta, \quad \eta \sim \mathcal{N}(0, 1). \quad (\text{C1})$$

Averaging over the distribution  $p(\Delta\theta|\theta)$ , the mean change is  $\langle\Delta\theta\rangle_{\Delta\theta\sim p(\Delta\theta|\theta)} = \mu(\theta)\Delta t$ , and the variance is  $\langle(\Delta\theta - \mu(\theta)\Delta t)^2\rangle_{\Delta\theta\sim p(\Delta\theta|\theta)} = 2D_c\Delta t$ . We can reproduce these with small finite jumps of  $\Delta\theta = \pm\alpha$ , with rates  $\beta_{\pm}(\theta)$ :

$$\begin{aligned} p(\pm\alpha|\theta) &= \beta_{\pm}(\theta)\Delta t \\ p(0|\theta) &= 1 - \sum_{\pm} \beta_{\pm}(\theta)\Delta t. \end{aligned}$$

Solving, we get

$$\beta_{\pm}(\theta) = \frac{D_c}{\alpha^2} \pm \frac{\mu(\theta)}{2\alpha} + \mathcal{O}(\Delta t). \quad (\text{C2})$$

Here we must assume  $D_c > \alpha|\mu(\theta)|/2 > 0$ .

Now we can plug these probabilities into the mutual information:

$$I(\Theta; \Delta\Theta) = \int d\theta \sum_{\pm} p(\pm\alpha|\theta)p(\theta) \log \frac{p(\pm\alpha|\theta)}{p(\pm\alpha)} + \mathcal{O}(\Delta t^2) \quad (\text{C3})$$

where the denominator is

$$p(\pm\alpha) = \int d\theta' p(\pm\alpha|\theta')p(\theta') = \left[ \frac{D_c}{\alpha^2} \pm \frac{\langle\mu\rangle}{2\alpha} \right] \Delta t + \mathcal{O}(\Delta t^2). \quad (\text{C4})$$

Then expanding at small  $\alpha$  we get

$$I(\Theta; \Delta\Theta) = \int d\theta p(\theta) \sum_{\pm} \left[ \frac{D_c}{\alpha^2} \pm \frac{\mu(\theta)}{2\alpha} \right] \log \frac{\frac{D_c}{\alpha^2} \pm \frac{\mu(\theta)}{2\alpha}}{\frac{D_c}{\alpha^2} \pm \frac{\langle\mu\rangle}{2\alpha}} + \dots \quad (\text{C5})$$

$$= \Delta t \int d\theta p(\theta) \frac{[\mu(\theta) - \langle\mu\rangle]^2}{4D_c} + \mathcal{O}(\alpha, \Delta t^2) \quad (\text{C6})$$

which is the desired formula, the first term of (3). The second term, for tumbles, can be derived in much the same way, taking  $p(\text{tumble}|\theta) = \lambda(\theta)\Delta t$  and expanding in  $\Delta t$  like (C3).

### C.2 Exact solution for steering $\mu(\theta)$

When  $\mu(\theta)$  has full freedom, we expect by symmetry that there will be no net rotational flux of the heading. In this case we can integrate the Fokker-Planck equation after setting the steady-state condition  $\partial_t p = 0$ , to obtain a Boltzmann-like solution of the form

$$p(\theta) = \frac{1}{Z} \exp\left(\frac{1}{D_r + D_c} \int \mu(\theta') d\theta'\right), \quad (\text{C7})$$

for partition function  $Z$  defined to ensure normalization. It follows then that the steering force can be written as a function of the probability distribution as

$$\mu(\theta) = (D_r + D_c)\partial_\theta \log p(\theta). \quad (\text{C8})$$

This allows us to write the information rate as a function only of  $p(\theta)$ , as

$$i = \frac{1}{4D_c} \text{Var}(\mu) \quad (\text{C9a})$$

$$= \frac{(D_r + D_c)^2}{4D_c} \int_0^{2\pi} p(\theta) [\partial_\theta \log p(\theta)]^2 d\theta. \quad (\text{C9b})$$

We can then write the objective function as a functional integral,

$$\mathcal{L} = \int_0^{2\pi} d\theta \underbrace{\left[ p(\theta) \cos \theta - \frac{\gamma(D_r + D_c)^2}{4D_c} p(\theta) [\partial_\theta \log p(\theta)]^2 + \alpha [p(\theta) - 1] \right]}_{f(\theta, p, p')}. \quad (\text{C10})$$

Here  $\alpha$  is a Lagrange multiplier ensuring normalization of  $p(\theta)$ . Assuming that  $\mu(\theta)$  has sufficient freedom to tune  $p(\theta)$  as needed for any  $D_c$ , we can optimize  $\mathcal{L}$  with respect to  $D_c$  at constant  $p(\theta)$ , which yields  $D_c = D_r$ . We then extremize  $\mathcal{L}$  by deriving the Euler-Lagrange equation, obtaining the following differential equation which  $p(\theta)$  must solve:

$$0 = \alpha + \cos \theta + \gamma D_r \left( \frac{p'(\theta)}{p(\theta)} \right)^2 + 2\gamma D_r \frac{d}{d\theta} \left( \frac{p'(\theta)}{p(\theta)} \right). \quad (\text{C11})$$

This differential equation falls within the Mathieu family, and can thus be solved exactly in closed form using special functions; after enforcing normalization and rotational symmetry this yields

$$p(\theta) = \frac{1}{\pi} \text{ce}_0(\theta/2, q)^2. \quad (\text{C12})$$

Here  $\text{ce}_0$  is the zeroth order Mathieu C function of the first kind [32], and  $q = -1/(2D_r\gamma)$  is a dimensionless parameter. This distribution is normalized and periodic on  $\theta \in [0, 2\pi]$ , with a peak at  $\theta = 0$  for  $\gamma > 0$ . We use the standard convention that  $\int_0^\pi \text{ce}_0(x, q)^2 dx = \pi$ . We will call  $p(\theta) = \frac{1}{\pi} \text{ce}_0(\theta/2, q)^2$  the Mathieu distribution. This distribution has previously been studied as the solution to some problems in quantum mechanics [33, 34]. The corresponding steering force is given by

$$\mu(\theta) = 4D_r \frac{\text{ce}'_0(\theta/2, q)}{\text{ce}_0(\theta/2, q)}. \quad (\text{C13})$$

### C.3 Pareto Frontier

For this steering strategy it is possible to evaluate both the average velocity and information rate in closed form using the Mathieu characteristic function  $a_0(q)$  and its derivative  $a'_0(q)$ . To do so, we first note that the Mathieu function  $y(x) = \text{ce}_0(x, q)$  satisfies the ODE

$$\underbrace{\left[ -\frac{d^2}{dx^2} + 2q \cos(2x) \right]}_{=H(q)} y = a_0(q)y, \quad (\text{C14})$$

where we have defined the operator  $H(q)$ , which we note is self-adjoint as a result of periodic boundary conditions. Taking a partial derivative with respect to  $q$ , multiplying both sides by  $y$ , and integrating over  $x$  from 0 to  $\pi$ , we obtain

$$\int_0^\pi y \frac{\partial H}{\partial q} y dx + \int_0^\pi y H(q) \frac{\partial y}{\partial q} dx = a'_0(q) \int_0^\pi y^2 dx + a_0(q) \int_0^\pi y \frac{\partial y}{\partial q} dx. \quad (\text{C15})$$

Using the self-adjoint nature of  $H$ , we can write

$$\int_0^\pi y H(q) \frac{\partial y}{\partial q} dx = \int_0^\pi H(q) y \frac{\partial y}{\partial q} dx \quad (\text{C16a})$$

$$= a_0(q) \int_0^\pi y \frac{\partial y}{\partial q} dx. \quad (\text{C16b})$$

This simplifies Eq. (C15) to

$$\int_0^\pi y \frac{\partial H}{\partial q} y dx = a'_0(q) \int_0^\pi y^2 dx. \quad (\text{C17})$$

Noting now that  $\partial H / \partial q = 2 \cos(2x)$ , we can simplify and rearrange this equation to yield

$$\frac{1}{2} a'_0(q) = \frac{\int_0^\pi \cos(2x) y^2 dx}{\int_0^\pi y^2 dx}. \quad (\text{C18})$$

Since our solution  $p(\theta) = y(\theta/2)^2 / \pi$ , the right hand side of this equation is exactly  $\langle \cos \theta \rangle$ , so that we have

$$\langle \cos \theta \rangle = \frac{1}{2} a'_0(q). \quad (\text{C19})$$

We then turn to evaluate the information rate  $i$ , which we can write in terms of  $y(x)$  as

$$i/D_r = \int_0^{2\pi} p(\theta) [\partial_\theta \ln p(\theta)]^2 d\theta \quad (\text{C20a})$$

$$= \frac{\int_0^\pi (y'(x))^2 dx}{\int_0^\pi y(x)^2 dx}. \quad (\text{C20b})$$

To evaluate this expression, we return to our original ODE for  $y$ , multiply both sides by  $y$ , and integrate from  $x = 0$  to  $\pi$  to obtain

$$\int_0^\pi y y'' dx + a_0(q) \int_0^\pi y^2 dx = 2q \int_0^\pi \cos(2x) y^2 dx. \quad (\text{C21})$$

Using our result (C18), we can simplify this to

$$q a'_0(q) - a_0(q) = \frac{\int_0^\pi y y'' dx}{\int_0^\pi y^2 dx}. \quad (\text{C22})$$

Using integration by parts to show  $\int y y'' = -\int y'^2$ , we can then relate the right-hand side to the information rate, for which we obtain

$$i/D_r = a_0(q) - q a'_0(q). \quad (\text{C23})$$

We thus have a parametric form of the Pareto frontier that can easily be evaluated numerically:

$$v/v_0 = \frac{1}{2} a'_0(q), \quad (\text{C24a})$$

$$i/D_r = a_0(q) - q a'_0(q). \quad (\text{C24b})$$

#### C.4 Approximations to the solution for steering $\mu(\theta)$

As has been noted previously [33, 34], the Mathieu distribution is well-approximated by a von-Mises distribution for both large and small  $q$ , which correspond to the low and high information limits respectively. The von-Mises distribution takes the form

$$p(\theta) = \frac{1}{2\pi I_0(\kappa)} \exp[\kappa \cos(\theta)], \quad (\text{C25})$$

with shape parameter  $\kappa$ .  $I_0(\kappa)$  is the 0'th order modified Bessel function of the first kind.

As  $q \rightarrow 0$  (low information) the Mathieu distribution is approximated by a von-Mises distribution with  $\kappa = -q$ , which leads to a steering strategy

$$\mu(\theta) \approx -\frac{1}{\gamma} \sin \theta. \quad (\text{C26})$$

With this steering strategy we obtain the scaling

$$v/v_0 \approx \sqrt{\frac{i/D_r}{2}}. \quad (\text{C27})$$

Conversely, as  $q \rightarrow -\infty$  (high information), the Mathieu distribution is approximated by a von-Mises distribution with  $\kappa = -\sqrt{-q}$ , leading to a steering strategy

$$\mu(\theta) \approx -\sqrt{\frac{2D_r}{\gamma}} \sin \theta, \quad (\text{C28})$$

and velocity-information scaling

$$v/v_0 \approx 1 - \frac{1}{2i/D_r}. \quad (\text{C29})$$

More generally, we find that the von-Mises ansatz for  $p(\theta)$  is a remarkably good approximation to the true optimal solution even at intermediate information rates. This functional form allows us to derive an implicit approximation for the Pareto frontier,

$$\frac{v}{v_0} = \frac{I_1\left(\frac{i/D_r}{v/v_0}\right)}{I_0\left(\frac{i/D_r}{v/v_0}\right)}, \quad (\text{C30})$$

with  $I_0$  and  $I_1$  the 0'th and first order modified Bessel function of the first kind

### C.5 Sign-only steering $\mu_{\text{left-right}}(\theta)$

For steering, perhaps the simplest solution uses only the sign of  $\theta$ , adopting a fixed steering rate left or right as required. This could be the case if, for example, the steering force is constrained to only take a single magnitude  $|M|$ , or if only the sign of  $\theta$  can be measured. Using only the sign of  $\theta$ , the control strategy must take on the following odd functional form:

$$\mu_{\text{left-right}}(\theta) = \begin{cases} -M, & 0 < \theta < \pi \\ M, & \text{else.} \end{cases} \quad (\text{C31})$$

We can solve for the resulting steady-state probability distribution, which is

$$p(\theta) = \frac{\exp\left(\frac{M(\pi-|\theta|)}{D_r+D_c}\right)}{2(D_r+D_c)\left(\exp\left(\frac{M\pi}{D}\right)-1\right)}. \quad (\text{C32})$$

The velocity and information rate are similarly analytically tractable, and are given by

$$v/v_0 = \frac{M^2 \coth\left(\frac{M\pi}{2(D_r+D_c)}\right)}{M^2 + (D_r+D_c)^2}, \quad (\text{C33a})$$

$$i = \frac{M^2}{4D_c}. \quad (\text{C33b})$$

Combining the two to eliminate  $M$ , we obtain the full Pareto frontier

$$v/v_0 = \frac{\coth\left(\frac{\pi}{2}\sqrt{\frac{i}{D_r}}\right)}{1 + \frac{D_r}{i}}. \quad (\text{C34})$$

For low information, the limiting behavior is

$$v/v_0 \sim \frac{2}{\pi} \sqrt{i/D_r}, \quad (\text{C35})$$

while at high information we have

$$v/v_0 \sim 1 - \frac{D_r}{i}. \quad (\text{C36})$$

At low information, this has performance only slightly below that of the full solution (coefficient  $2/\pi \approx 0.64$  vs.  $1/\sqrt{2} \approx 0.71$ ), while at high information, it needs twice as much information to obtain the same velocity.

### C.6 Steering without sign $\mu(|\theta|)$ , at low information rate

We now consider a more constrained case of the continuous steering problem, where the drift  $\mu(\theta)$  is required to be an even function of  $\theta$ . In this case the steady-state distribution no longer takes the Boltzmann form, and there may generally be a net circular flux  $J$ . The FPE is (setting  $D = D_c + D_r$ )

$$J = -\mu(\theta)p(\theta) + Dp'(\theta). \quad (\text{C37})$$

Integrating once more reveals that  $2\pi J = -\langle \mu \rangle$ . Solving for  $\mu(\theta)$  as a function of  $p(\theta)$ , we have

$$\mu(\theta) = -\frac{J}{p(\theta)} + D \frac{p'(\theta)}{p(\theta)}. \quad (\text{C38})$$

We expand around the low information limit, where  $\mu$  and  $p(\theta)$  are both constant so that up-gradient velocity is zero. For large  $\gamma$  and requiring  $\mu(\theta)$  to take the form of a cosine series to enforce evenness, we obtain

$$\mu(\theta) = \pm 2D_r \mp \frac{1}{2\gamma} \cos(\theta). \quad (\text{C39a})$$

The corresponding velocity and information rate are

$$v/v_0 = \frac{1}{16\gamma D_r}, \quad (\text{C40a})$$

$$i = \frac{1}{32\gamma^2 D_r}, \quad (\text{C40b})$$

so that the final scaling is

$$\frac{v}{v_0} = \sqrt{\frac{i}{8D_r}}. \quad (\text{C41})$$

We can also compute the average velocity perpendicular to the gradient, which we find is equal in magnitude to the up-gradient velocity.

## Appendix D. Discreteness of the optimal target distribution

For this section, we consider arbitrary jumping strategies. These are specified by the jump rate  $\lambda(\theta)$  and the target jump distributions  $q_\theta(\Delta\theta)$ . While we are allowing the distributions to vary over  $\theta$ , we focus on the case of symmetric jump distributions, such that  $q_\theta(\Delta\theta) = q_\theta(-\Delta\theta)$ . Under this specification, the master equation becomes

$$\frac{dp(\theta)}{dt} = -\lambda(\theta)p(\theta) + \int d\Delta\theta \lambda(\theta - \Delta\theta)p(\theta - \Delta\theta)q_{\theta-\Delta\theta}(\Delta\theta) + D_r p''(\theta). \quad (\text{D1})$$

Using the above master equation as a constraint, our optimization problem can be written as the following augmented problem:

$$\max_{p, \lambda, (q_\theta)_\theta} \int d\theta p(\theta) \cos(\theta) - \gamma i \quad \text{s.t.} \quad -\lambda(\theta)p(\theta) + \int d\Delta\theta \lambda(\theta - \Delta\theta)p(\theta - \Delta\theta)q_\theta(\Delta\theta) + D_r p''(\theta) = 0 \quad \forall \theta, \quad (\text{D2})$$

where  $p$  and  $q_\theta$  are subject to normalization constraints, the distributions  $q_\theta$  are symmetric, and all choice variables are non-negative.

To invoke some useful results from measure theory, it is convenient to write the target distributions in terms of their corresponding measures. Let  $Q_\theta$  be the measure associated to the target distribution at  $\theta$ , such that

$$dQ_\theta(\Delta\theta) = q_\theta(\Delta\theta) d\Delta\theta. \quad (\text{D3})$$

Now, let  $\langle \lambda \rangle := \int d\theta p(\theta)\lambda(\theta)$ . Note that  $p(\theta)\lambda(\theta)/\langle \lambda \rangle$  is the density of the distribution of locations where jumps are originated. Therefore, the probability of jump sizes averaged over jump sources is captured by the mixture  $\bar{Q}$ :

$$\bar{Q} := \frac{1}{\langle \lambda \rangle} \int d\theta p(\theta)\lambda(\theta)Q_\theta. \quad (\text{D4})$$

Let us denote the collection of target measures with  $\mathbf{Q} := (Q_\theta)_\theta$ . We can write our information rate in terms of  $(p, \lambda, \mathbf{Q})$  as

$$i(p, \lambda, \mathbf{Q}) = \int d\theta p(\theta)\lambda(\theta) \left[ \log \left( \frac{\lambda(\theta)}{\langle \lambda \rangle} \right) + D_{\text{KL}}(Q_\theta \| \bar{Q}) \right] \quad (\text{D5})$$

In terms of the target measures, the Lagrangian of the problem (D2) is

$$\begin{aligned} \mathcal{L}_1(p, \lambda, \mathbf{Q}) = & \int d\theta p(\theta) [\cos(\theta) + D_r \chi''(\theta) + \psi_p] \\ & + \int d\theta p(\theta)\lambda(\theta) \left[ -\gamma \log \left( \frac{\lambda(\theta)}{\langle \lambda \rangle} \right) - \gamma D_{\text{KL}}(Q_\theta \| \bar{Q}) + \int dQ_\theta(\Delta\theta) \chi(\theta + \Delta\theta) - \chi(\theta) \right], \end{aligned} \quad (\text{D6})$$

where  $\psi_p$  is the Lagrange multiplier that enforces the normalization of  $p$  and  $\chi(\theta)$  enforces the master equation constraint. We now separate the problem of optimization over target measures  $\mathbf{Q}$  and optimization over  $(p, \lambda)$ .

### D.1 Optimization over target measures

For fixed  $p$  and  $\lambda$ , we can focus on the elements of the Lagrangian  $\mathcal{L}_1$  that depend on the measures  $\mathbf{Q}$ . This inner problem is similar to the one studied in [12] in the context of rational inattention.

Within  $\mathcal{L}_1$ , the only parts that depend on  $\mathbf{Q}$  can be grouped into the following ‘‘inner’’ Lagrangian:

$$\mathcal{L}_2(\mathbf{Q}) := \int d\theta p(\theta)\lambda(\theta) \left[ \int dQ_\theta(\Delta\theta) \chi(\theta + \Delta\theta) - \gamma D_{\text{KL}}(Q_\theta \| \bar{Q}) \right]. \quad (\text{D7})$$

Therefore, for a fixed  $p$  and  $\lambda$ , optimizing  $\mathcal{L}_1$  over  $\mathbf{Q}$  is equivalent to solving

$$\max_{\mathbf{Q}} \mathcal{L}_2(\mathbf{Q}) \quad \text{subject to } Q_\theta \text{ symmetric } \forall \theta. \quad (\text{D8})$$

As we show in Section D6, this problem is equivalent to solving the following augmented problem:

$$\max_{\mathbf{Q}, R} \mathcal{L}'_2(\mathbf{Q}, R), \quad (\text{D9})$$

where now  $(Q_\theta)_\theta$  and  $R$  are unrestricted probability measures, and we have defined the augmented Lagrangian

$$\mathcal{L}'_2(\mathbf{Q}, R) := \int d\theta p(\theta)\lambda(\theta) \left[ \frac{1}{2} \int dQ_\theta(\Delta\theta) [\chi(\theta + \Delta\theta) + \chi(\theta - \Delta\theta)] - \gamma D_{\text{KL}}(Q_\theta \| R) \right]. \quad (\text{D10})$$

As we will show, at the optimum this problem satisfies  $R^* = \bar{Q}^*$ , which is necessary for these problems to be equivalent.

Let us first do the optimization in (D9) over the measures  $\mathbf{Q}$ . Note that this can be done independently for each  $\theta$  by solving the problem

$$\max_{Q_\theta} \mathcal{L}_\theta(Q_\theta), \quad \mathcal{L}_\theta(Q_\theta) := \frac{1}{2} \int dQ_\theta(\Delta\theta) [\chi(\theta + \Delta\theta) + \chi(\theta - \Delta\theta)] - \gamma D_{\text{KL}}(Q_\theta \| R). \quad (\text{D11})$$

Using the Donsker-Varadhan variational formula for the KL divergence, this problem can be solved in closed form. The unique maximizer (given  $R$ )  $Q_{\theta,R}^*$  satisfies

$$dQ_{\theta,R}^*(\Delta\theta) = \frac{e^{[\chi(\theta+\Delta\theta)+\chi(\theta-\Delta\theta)]/2\gamma}}{Z_R(\theta)} dR(\Delta\theta). \quad (\text{D12})$$

Furthermore, the value of our objective function is

$$\mathcal{L}_\theta(Q_{\theta,R}^*) = \gamma \log \left( \underbrace{\int dR(\Delta\theta) e^{\frac{1}{2\gamma}[\chi(\theta+\Delta\theta)+\chi(\theta-\Delta\theta)]}}_{=: Z_R(\theta)} \right). \quad (\text{D13})$$

Using the solution to our optimization of  $\mathcal{L}_\theta$ , we can return to the problem (D9) and maximize over  $R$ . Note that

$$\mathcal{L}'_2(\mathbf{Q}_R^*, R) = \int d\theta p(\theta)\lambda(\theta) \mathcal{L}_\theta(Q_{\theta,R}^*) = \gamma \int d\theta p(\theta)\lambda(\theta) \log(Z_R(\theta)). \quad (\text{D14})$$

Therefore, our optimization over  $R$  is

$$\max_R \mathcal{L}'_2(\mathbf{Q}_R, R) = \max_R \left\{ \gamma \int d\theta p(\theta)\lambda(\theta) \log(Z_R(\theta)) \right\}. \quad (\text{D15})$$

In order to solve problem (D15), we use the technical result in Section D7 on optimization over measures. First, note that the functional  $\mathcal{L}'_2(\mathbf{Q}_R, R)$  is concave, since  $R$  enters linearly into the logarithm. We also have the following functional derivative (letting  $r(\Delta\theta)$  be the density of  $R$ ):

$$\frac{\delta \mathcal{L}'_2(\mathbf{Q}_R, R)}{\delta r(\Delta\theta)} = \gamma \int d\theta p(\theta)\lambda(\theta) \frac{e^{[\chi(\theta+\Delta\theta)+\chi(\theta-\Delta\theta)]/2\gamma}}{Z_R(\theta)} =: \gamma \langle \lambda \rangle \Psi_R(\Delta\theta). \quad (\text{D16})$$

The function  $\Psi_R$  is called the *contact function*, and it determines the support of the optimizer. Using the result in Section D7, we have that there exists a constant  $\kappa$  such that, at the optimizer  $R^*$ ,

$$\gamma \langle \lambda \rangle \Psi_{R^*}(\Delta\theta) \leq \kappa \quad \forall \Delta\theta, \quad \gamma \langle \lambda \rangle \Psi_{R^*}(\Delta\theta) = \kappa \quad \forall \Delta\theta \in \text{supp}(R^*). \quad (\text{D17})$$

Integrating the second equality against  $R^*$  and using Eq. (D12) implies that  $\kappa = \gamma \langle \lambda \rangle$ . Therefore, our contact conditions are

$$\Psi_{R^*}(\Delta\theta) \leq 1 \quad \forall \Delta\theta, \quad \Psi_{R^*}(\Delta\theta) = 1 \quad \forall \Delta\theta \in \text{supp}(R^*). \quad (\text{D18})$$

We can now confirm that this solution satisfies  $R^* = \bar{Q}^*$ . Using the solution in Eq. (D12), we see that the density of  $Q^*$  is

$$\begin{aligned} d\bar{Q}^*(\Delta\theta) &= \frac{1}{\langle \lambda \rangle} \int d\theta p(\theta)\lambda(\theta) dQ_\theta^*(\Delta\theta) \\ &= \frac{1}{\langle \lambda \rangle} \int d\theta p(\theta)\lambda(\theta) \frac{e^{[\chi(\theta+\Delta\theta)+\chi(\theta-\Delta\theta)]/2\gamma}}{Z_{R^*}(\theta)} dR^*(\Delta\theta) \\ &= \Psi_{R^*}(\Delta\theta) dR^*(\Delta\theta). \end{aligned} \quad (\text{D19})$$

Using our contact conditions, we know that  $\Psi_{R^*} = 1$  for all  $\Delta\theta$  in the support of  $R^*$ . Thus, we have  $\bar{Q}^* = R^*$ .

Having characterized the optimal target measures, we can return to the optimization over  $p$  and  $\lambda$ .

## D.2 Optimization over $p$ and $\lambda$

Now we consider fixed  $\chi$  and  $\mathbf{Q}$ , and optimize the original Lagrangian (D6) over  $p$  and  $\lambda$ . Optimizing over  $\lambda$  yields

$$\frac{\delta \mathcal{L}_1(p, \lambda, \mathbf{Q})}{\delta \lambda(\theta)} = p(\theta) \left\{ -\gamma \log \left( \frac{\lambda(\theta)}{\langle \lambda \rangle} \right) - \gamma D_{\text{KL}}(Q_\theta \| \bar{Q}) + \int dQ_\theta(\Delta\theta) \chi(\theta + \Delta\theta) - \chi(\theta) \right\} = 0. \quad (\text{D20})$$

Similarly, optimizing over  $p$  gives

$$\begin{aligned} \frac{\delta \mathcal{L}_1(p, \lambda, \mathbf{Q})}{\delta p(\theta)} &= \cos(\theta) - \gamma \lambda(\theta) \left[ \log \left( \frac{\lambda(\theta)}{\langle \lambda \rangle} \right) + D_{\text{KL}}(Q_\theta \| \bar{Q}) - 1 \right] + \psi_p + D_r \chi''(\theta) \\ &\quad + \lambda(\theta) \left[ \int dQ_\theta(\Delta\theta) \chi(\theta + \Delta\theta) - \chi(\theta) \right] = 0. \end{aligned} \quad (\text{D21})$$

Combining these two first-order conditions yields the following second-order differential equation for  $\chi$ :

$$D_r \chi''(\theta) + \psi_p + \cos(\theta) + \gamma \lambda(\theta) = 0. \quad (\text{D22})$$

Integrating over  $[-\pi, \pi]$  and using periodicity yields

$$\psi_p = -\gamma \underbrace{\frac{1}{2\pi} \int d\theta \lambda(\theta)}_{=: \lambda_0}. \quad (\text{D23})$$

Therefore, the differential equation for  $\chi$  is fully characterized by  $\lambda$ :

$$D_r \chi''(\theta) + \cos(\theta) + \gamma[\lambda(\theta) - \lambda_0] = 0. \quad (\text{D24})$$

Additionally, note that for symmetric measures  $\mathbf{Q}$ , the first-order condition for  $\lambda$  can be written as

$$-\gamma \log \left( \frac{\lambda(\theta)}{\langle \lambda \rangle} \right) - \gamma D_{\text{KL}}(Q_\theta \| \bar{Q}) + \frac{1}{2} \int dQ_\theta(\Delta\theta) [\chi(\theta + \Delta\theta) + \chi(\theta - \Delta\theta)] - \chi(\theta) = 0 \quad (\text{D25})$$

Together, Equations (D24) and (D25) capture the structure of the optimal  $p$  and  $\lambda$ . We can now put together the  $\mathbf{Q}$  and  $(p, \lambda)$  optimizations.

## D.3 Joint optimization

Under the optimal measures  $Q_\theta^*$ , following Eq. (D12), the Donsker-Varadhan result gave us

$$\frac{1}{2} \int dQ_\theta^*(\Delta\theta) [\chi(\theta + \Delta\theta) + \chi(\theta - \Delta\theta)] - \gamma D_{\text{KL}}(Q_\theta^* \| \bar{Q}^*) = \gamma \log(Z_{\bar{Q}^*}(\theta)). \quad (\text{D26})$$

Comparing with Equation (D25), we get

$$Z_{\bar{Q}^*}(\theta) = \frac{\lambda(\theta)}{\langle \lambda \rangle} e^{\chi(\theta)/\gamma}. \quad (\text{D27})$$

This implies that our contact function at the optimum is

$$\Psi_{\bar{Q}^*}(\Delta\theta) = \int d\theta p(\theta) e^{[\chi(\theta + \Delta\theta) + \chi(\theta - \Delta\theta) - 2\chi(\theta)]/2\gamma}. \quad (\text{D28})$$

We are now ready to prove that the optimal target measures are discrete.

#### D.4 Discreteness of target support

To show discreteness of the distribution of targets, we show that the contact function can only equal 1 at a finite number of points. We do this by showing that it is analytic and non-constant, as has been done to show discreteness of optimal priors [9].

Now we evaluate all quantities at the optimum. To simplify notation, we define  $\Psi := \Psi_{\bar{Q}^*}$ . First, note that  $\chi$  solves the ODE in equation (D24). For solutions with analytic  $\lambda$  (which we implicitly constrain our optimization to), this implies that  $\chi$  is analytic. Since  $e^x$  is an analytic function, it follows that  $\Psi$  is analytic in  $\Delta\theta$ .

Now, note that

$$\Psi''(0) = \frac{1}{\gamma} \int d\theta p(\theta) \chi''(\theta). \quad (\text{D29})$$

Taking the master equation (D1), multiplying by  $\chi(\theta)$  and integrating yields

$$D_r \int d\theta p(\theta) \chi''(\theta) + \int d\theta p(\theta) \lambda(\theta) \left[ \int dQ_\theta(\Delta\theta) \chi(\theta + \Delta\theta) - \chi(\theta) \right] = 0. \quad (\text{D30})$$

Using the first-order condition for  $\lambda$  (D20), we can rewrite the second integral as

$$D_r \int d\theta p(\theta) \chi''(\theta) + \gamma \int d\theta p(\theta) \lambda(\theta) \left[ \log \left( \frac{\lambda(\theta)}{\langle \lambda \rangle} \right) + D(Q_\theta \| \bar{Q}) \right] = 0. \quad (\text{D31})$$

Note that this second term is simply the information rate. Therefore,

$$\Psi''(0) = \int d\theta p(\theta) \chi''(\theta) = -\frac{\gamma}{D_r} i < 0, \quad (\text{D32})$$

since for finite  $\gamma$  the solution achieves a strictly positive information rate. Therefore,  $\Psi$  is not constant. Along with analyticity, this means that the contact condition  $\Psi(\Delta\theta) = 1$  can only hold at a finite number of points. Thus, the support of the distribution of targets at the optimum must be discrete.

#### D.5 Contact function for steering strategies

As with jumping strategies, the optimal steering problem can also be formulated in terms of an optimization problem over  $p$ ,  $\mu$  and  $D_c$ , where the master equation is enforced through the Lagrange multiplier  $\chi(\theta)$ . The Lagrangian for the steering problem is

$$\mathcal{L}_{\text{steering}}(p, \mu, D_c) = \int d\theta p(\theta) \left[ \cos(\theta) - \frac{\gamma}{4D_c} [\mu(\theta) - \langle \mu \rangle]^2 + \psi_p \right] + \int d\theta \chi(\theta) \left[ (D_r + D_c) p''(\theta) - \frac{d}{d\theta} (\mu(\theta) p(\theta)) \right], \quad (\text{D33})$$

where  $\psi_p$  enforces the normalization constraint for  $p$ . For a fixed  $\chi$ , the optimization problem can be re-written as

$$\max_{p, \mu, D_c} \int d\theta p(\theta) \left\{ \cos(\theta) - \frac{\gamma}{4D_c} [\mu(\theta) - \langle \mu \rangle]^2 + \psi_p + (D_r + D_c) \chi''(\theta) + \mu(\theta) \chi'(\theta) \right\}. \quad (\text{D34})$$

The first-order condition for  $\mu$  is

$$\frac{\delta \mathcal{L}_{\text{steering}}(p, \mu, D_c)}{\delta \mu(\theta)} = p(\theta) \chi'(\theta) - \frac{\gamma}{2D_c} p(\theta) [\mu(\theta) - \langle \mu \rangle] = 0. \quad (\text{D35})$$

Here we can invoke the solution to the problem from Section C2. We have  $D_c^* = D_r$ ,  $\langle \mu \rangle = 0$  and  $\mu(\theta) = 2\partial_\theta \log(p(\theta))$ . Using this in our differential equation for  $\chi$  yields

$$\chi'(\theta) = \gamma \partial_\theta \log(p(\theta)) \quad \implies \quad \frac{\chi(\theta)}{\gamma} = \log(p(\theta)) + c_0, \quad (\text{D36})$$

for some constant  $c_0$ .

Since the contact function for jump strategies in Section D 3 only depends on the Lagrange multiplier  $\chi$ , we can evaluate it for the steering case. For jumping strategies with non-symmetric targets  $Q_\theta$ , the contact function would be

$$\Psi(\Delta\theta) = \int d\theta p(\theta) e^{[\chi(\theta+\Delta\theta) - \chi(\theta)]/\gamma}. \quad (\text{D37})$$

With our solution for  $\chi$  in the steering case, we can evaluate the contact function to be

$$\Psi(\Delta\theta) = \int d\theta p(\theta + \Delta\theta) = 1. \quad (\text{D38})$$

## D.6 Equivalence of the augmented optimization problem

Let us consider the problem

$$\begin{aligned} \max_{\mathbf{Q}} \mathcal{L}_2(\mathbf{Q}) \quad \text{subject to } Q_\theta \text{ symmetric } \forall \theta, \\ \mathcal{L}_2(\mathbf{Q}) := \int d\theta p(\theta) \lambda(\theta) \left[ \int dQ_\theta(\Delta\theta) \chi(\theta + \Delta\theta) - \gamma D_{\text{KL}}(Q_\theta \| \bar{Q}) \right], \end{aligned} \quad (\text{D39})$$

Since we are considering symmetric measures, we can re-write the objective function as

$$\mathcal{L}_2(\mathbf{Q}) = \int d\theta p(\theta) \lambda(\theta) \left[ \frac{1}{2} \int dQ_\theta(\Delta\theta) [\chi(\theta + \Delta\theta) + \chi(\theta - \Delta\theta)] - \gamma D_{\text{KL}}(Q_\theta \| \bar{Q}) \right]. \quad (\text{D40})$$

We will now prove that the problem above can be solved with symmetric measures, even when the symmetry constraint is lifted. When the symmetry constraint is lifted, the space of admissible measures is expanded, so if the solution of the expanded problem is symmetric, it will also be a solution of the constrained problem. That is, we now consider the problem

$$\max_{\mathbf{Q}} \mathcal{L}_2(\mathbf{Q}). \quad (\text{D41})$$

Consider an arbitrary collection  $\mathbf{Q}$  (not necessarily symmetric). We will prove that symmetrizing it weakly improves the objective function. Define the symmetrized measures

$$Q_\theta^s := \frac{1}{2}(Q_\theta + Q_\theta^-), \quad (\text{D42})$$

where  $Q_\theta^-$  is the measure obtained under the transformation  $\Delta\theta \rightarrow -\Delta\theta$ . Clearly these measures satisfy

$$\int dQ_\theta(\Delta\theta) [\chi(\theta + \Delta\theta) + \chi(\theta - \Delta\theta)] = \int dQ_\theta^s(\Delta\theta) [\chi(\theta + \Delta\theta) + \chi(\theta - \Delta\theta)]. \quad (\text{D43})$$

Therefore, the first part of the objective is unchanged under symmetrization. Additionally, using the convexity of the KL divergence, we have that

$$D_{\text{KL}}(Q_\theta^s \| \bar{Q}^s) \leq D_{\text{KL}}(Q_\theta \| \bar{Q}) \quad \forall \theta. \quad (\text{D44})$$

This means that symmetrizing the measures weakly improves the objective:

$$\mathcal{L}_2(\mathbf{Q}^s) \geq \mathcal{L}_2(\mathbf{Q}) \quad \forall \mathbf{Q}. \quad (\text{D45})$$

Therefore, if a non-symmetric solution exists, it can always be symmetrized to weakly improve the objective. We can, then, find our optimal measures by solving the unconstrained problem.

To make progress, we again augment the problem by optimizing over an additional probability measure  $R$ :

$$\max_{\mathbf{Q}, R} \mathcal{L}'_2(\mathbf{Q}, R), \quad (\text{D46})$$

where the augmented Lagrangian is

$$\mathcal{L}'_2(\mathbf{Q}, R) := \int d\theta p(\theta) \lambda(\theta) \left[ \frac{1}{2} \int dQ_\theta(\Delta\theta) [\chi(\theta + \Delta\theta) + \chi(\theta - \Delta\theta)] - \gamma D_{\text{KL}}(Q_\theta \| R) \right]. \quad (\text{D47})$$

Note that this augmented Lagrangian satisfies

$$\mathcal{L}'_2(\mathbf{Q}, \bar{Q}) = \mathcal{L}_2(\mathbf{Q}). \quad (\text{D48})$$

This means that our search space reaches all possible values of the optimization problem (D41). Now, suppose a solution to (D46) problem exists that satisfies

$$R^* = \frac{1}{\langle \lambda \rangle} \int d\theta p(\theta) \lambda(\theta) Q_\theta^* = \bar{Q}^*. \quad (\text{D49})$$

This would imply that  $\mathbf{Q}^*$  also solves (D41). This condition is verified in (D19), so our augmented problem (D46) also solves our original problem (D39).

## D.7 Optimization over measures

In this section, we prove a technical result about the support of the solution when optimizing over measures.

**Lemma.**— Let  $\mathcal{X}$  be a compact metric space and  $\mathcal{P}(\mathcal{X})$  be the set of probability measures over  $\mathcal{X}$ . Suppose the function  $F : \mathcal{P}(\mathcal{X}) \rightarrow \mathbb{R}$  is concave and that there exists  $f : \mathcal{P}(\mathcal{X}) \times \mathcal{X} \rightarrow \mathbb{R}$  such that

$$\left. \frac{d}{dt} F((1-t)\mu + t\nu) \right|_{t=0^+} = \int_{\mathcal{X}} f_\mu(x) d(\nu - \mu)(x). \quad (\text{D50})$$

Additionally, suppose  $f$  is continuous on  $x$  for all  $\mu$ . Then for any  $\mu^*$  that solves the problem

$$\max_{\mu \in \mathcal{P}(\mathcal{X})} F(\mu) \quad (\text{D51})$$

there exists a constant  $\kappa$  such that

$$f_{\mu^*}(x) \leq \kappa \quad \forall x \in \mathcal{X}, \quad f_{\mu^*}(x) = \kappa \quad \forall x \in \text{supp}(\mu^*). \quad (\text{D52})$$

*Proof.* Fix  $\nu \in \mathcal{P}(\mathcal{X})$  and a maximizer  $\mu^*$ . Define the function  $\phi : [0, 1] \rightarrow \mathbb{R}$  as

$$\phi(t) := F((1-t)\mu^* + t\nu). \quad (\text{D53})$$

By concavity of  $F$ , the function  $\phi$  is concave. Additionally, since  $\mu^*$  is a maximizer of  $F$ , we have that  $\phi$  must attain its maximum at  $t = 0$ . For a concave function that attains its maximum at its left endpoint, we must have  $\phi'(0^+) \leq 0$ . By Eq. (D50), this implies that

$$\int_{\mathcal{X}} f_{\mu^*}(x) d\nu(x) \leq \int_{\mathcal{X}} f_{\mu^*}(x) d\mu^*(x) =: \kappa. \quad (\text{D54})$$

Note that this bound holds for arbitrary measures. In particular, taking the Dirac measure at  $x_0$ ,

$$\int_{\mathcal{X}} f_{\mu^*}(x) d\delta_{x_0}(x) = f_{\mu^*}(x_0) \leq \kappa. \quad (\text{D55})$$

Additionally, note that the maximum over  $\nu$  of  $\int_{\mathcal{X}} f_{\mu^*}(x) d\nu(x)$  is attained when the measure  $\nu$  concentrates its mass on the maxima of  $f_{\mu^*}$ . Since the inequality in Eq. (D54) holds for all  $\nu$ , it must be the case that  $\mu^*$  attains this maximum, so it must also concentrate its mass on the maxima of  $f_{\mu^*}$ . This implies that

$$\kappa = \int_{\mathcal{X}} f_{\mu^*}(x) d\mu^*(x) = \max_{x \in \mathcal{X}} f_{\mu^*}(x). \quad (\text{D56})$$

Therefore, we must have  $f_{\mu^*}(x) = \kappa$   $\mu^*$ -almost everywhere. Since  $f_{\mu^*}$  is continuous, this implies the stronger result that  $f_{\mu^*}(x) = \kappa$  for all  $x \in \text{supp}(\mu^*)$ .  $\square$

The result above generalizes the usual KKT conditions for constrained optimization to the case of measures. Here, the inequality  $f_{\mu^*}(x) \leq \kappa$  ensures the non-negativity constraint of the measure. For points on the support, the constraint is slack, and the constraint binds for all points where the inequality is strict.

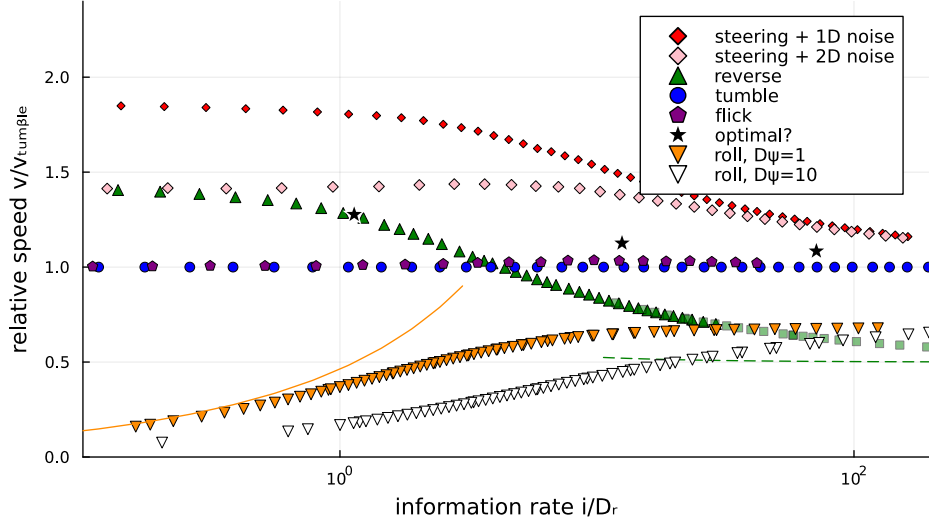


**Figure S4:** Performance of strategies for three-dimensional navigation, relative to tumbling. Red and pink diamonds show continuous steering with directional information for both “1D noise” (red) and “2D noise” (pink). Green triangles, blue circles, and purple pentagons respectively show the reverse, tumble, and flick strategies, while black stars indicate the optimal discrete strategy with only scalar information. Inverted triangles show scalar steering with roll diffusion, with  $D_\psi = D_r$  (orange) and  $D_\psi = 10D_r$  (white). Green dashed line shows the asymptotic scaling of the tumble strategy in the high information limit, while the orange solid line shows the conjectured scaling of the unsigned steering strategy in the low information limit.

## Appendix E. Navigation in three or more dimensions

In the main text we briefly discussed how the navigation problem and resulting optimal strategies change in three dimensions. Here we provide the details.

### E.1 Simple strategies in $d = 3$

Allowing steering and tumbles, the Fokker-Planck equation on the sphere of possible headings reads

$$\frac{dp}{dt} = \vec{\nabla} \cdot (\vec{\mu}p) - \lambda p + \langle \lambda \rangle + D \nabla^2 p. \quad (\text{E1})$$

Assuming radial symmetry  $p(\theta, \phi) = p(\theta)$ , and allowing complete tumbles, where the new heading is uniform on the sphere, we have:

$$\frac{dp(\theta)}{dt} = \underbrace{\int d\theta' \sin \theta' p(\theta') \lambda(\theta') - \lambda(\theta) p(\theta)}_{\text{tumbles}} + \underbrace{D_r \frac{1}{\sin \theta} \frac{d}{d\theta} \left[ \sin \theta \frac{dp(\theta)}{d\theta} \right]}_{\text{diffusion}}. \quad (\text{E2})$$

The simplest kind of steering is only towards or away from the North pole ( $\theta = 0$ ). The appropriate controller noise  $D_c$  is one-dimensional diffusion along the line of latitude,  $\frac{d}{dt}(\sin \theta p(\theta)) = D_c \frac{d^2}{d\theta^2}(\sin \theta p(\theta))$ . This leads to the following Fokker-Planck equation:

$$\frac{dp(\theta)}{dt} = \frac{1}{\sin \theta} \frac{d}{d\theta} [\sin \theta \mu(\theta) p(\theta)] + \frac{1}{\sin \theta} \frac{d}{d\theta} \left[ (D_r + D_c) \sin \theta \frac{dp(\theta)}{d\theta} + D_c \cos \theta p(\theta) \right]. \quad (\text{E3})$$

This is described as “1D noise” on the figures, and gives the red points in figure 4 in the main text. But another, simpler, choice of controller noise is to add another term exactly like the rotational diffusion term  $D_r$ :

$$\frac{dp(\theta)}{dt} = \frac{1}{\sin \theta} \frac{d}{d\theta} [\sin \theta \mu(\theta) p(\theta)] + \frac{1}{\sin \theta} \frac{d}{d\theta} \left[ (D_r + D_c) \sin \theta \frac{dp(\theta)}{d\theta} \right]. \quad (\text{E4})$$

This choice is described as “2D noise” on the figures, and the resulting pink points have slightly lower performance.

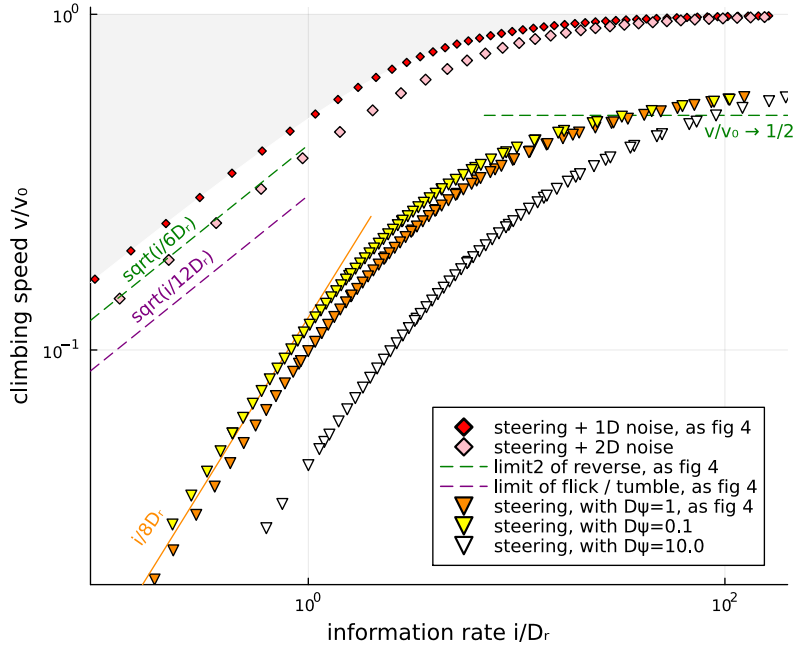


**Figure S5:** More results for 3D steering strategies, with velocity normalized by the maximum swimming speed. Red and pink diamonds show continuous steering with directional information for both “1D noise” (red) and “2D noise” (pink). Inverted triangles show scalar steering with roll diffusion, with  $D_\psi = D_r$  (orange),  $D_\psi = 0.1D_r$  (yellow), and  $D_\psi = 10D_r$  (white). Green and purple dashed lines show the low- and high-information scaling for tumble and flick respectively, while the orange solid line shows the conjectured low-information scaling for scalar steering.

We could also allow for both reversing the heading at rate  $\zeta(\theta)$  and 90 degree flicks at rate  $\kappa(\theta)$ . The sink terms are identical, but the source term involves an integral around a circle perpendicular to the original heading vector. Integrating out the azimuthal angle  $\phi$ , we obtain:

$$\frac{dp(\theta)}{dt} = \text{previous} - \underbrace{\zeta(\theta)p(\theta) + \zeta(\theta)p(\pi - \theta)}_{\text{reverse with rate } \zeta} - \underbrace{\kappa(\theta)p(\theta) + \frac{1}{2\pi} \int_0^{2\pi} d\psi \kappa(\theta'(\psi, \theta))p(\theta'(\psi, \theta))}_{\text{flick with rate } \kappa} \quad (\text{E5})$$

where  $\theta'(\psi, \theta) = \arccos(-\cos \psi \sin \theta)$ .

Figures S4 and S5 shows the performance trade-off curves for several of these strategies, computed from numerical solutions to the Fokker-Planck equation. As with the two-dimensional case we find that directed steering is optimal, although now the choice between (E3) and (E4) gives two different results. Among strategies not using the direction, The reverse strategy performs well in the low information limit, scaling as  $v/v_0 \approx \sqrt{i/6D_r}$ . Both tumble and flick perform worse, scaling in the low information limit as  $v/v_0 \approx \sqrt{i/12D_r}$ , but both outperform reverse at high information. The reverse strategy reaches a maximum velocity of  $v/v_0 = 1/2$  at high information, while the flick and tumble strategies reach  $v/v_0 = 1$  in the same limit.

## E.2 Information rate for steering in $d$ dimensions

While the generalization of the information rate is straightforward for discrete jumps, the generalization for continuous steering is somewhat more involved. Here we derive the information rate for the full  $d$ -dimensional version of the navigation problem. With only continuous steering, the dynamics for the heading vector  $\mathbf{n}$  on the  $d - 1$  dimensional sphere are

$$\dot{\mathbf{n}} = \boldsymbol{\mu}(\mathbf{n}) + \sqrt{2(D_r + D_c)}\boldsymbol{\eta}(t), \quad (\text{E6})$$

with  $|\mathbf{n}| = 1$  enforced for all  $t$ . Note that here we make the choice of “2D noise” as described in the previous section. The steering force  $\boldsymbol{\mu}$  resides in the  $d - 1$  dimensional space tangent to the  $d - 1$  sphere at the point  $\mathbf{n}$ , as does the random force  $\boldsymbol{\eta}(t)$ .

We are interested in computing the information rate

$$i = \lim_{dt \rightarrow 0} \frac{I[\mathbf{n}; \Delta_{\mathbf{c}} \mathbf{n}]}{dt}, \quad (\text{E7})$$

where

$$\Delta_{\mathbf{c}} \mathbf{n} := \boldsymbol{\mu}(\mathbf{n}) dt + \sqrt{2D_c dt} \boldsymbol{\eta}(t), \quad (\text{E8})$$

where  $\boldsymbol{\eta}$  has mean 0 and covariance given by the  $d-1$  dimensional identity matrix  $1_{d-1}$ . We then rescale this variable to a zero-mean variant,

$$\mathbf{z} := \frac{\Delta_{\mathbf{c}} \mathbf{n} - \langle \boldsymbol{\mu} \rangle_{p(\mathbf{n})} dt}{\sqrt{2D_c dt}}, \quad (\text{E9})$$

whose distribution conditional on  $\mathbf{n}$  satisfies

$$p(\mathbf{z}|\mathbf{n}) = \mathcal{N} \left[ \sqrt{\frac{dt}{2D_c}} (\boldsymbol{\mu}(\mathbf{n}) - \langle \boldsymbol{\mu} \rangle_{p(\mathbf{n})}), 1_{d-1} \right]. \quad (\text{E10})$$

The marginal distribution  $p(\mathbf{z})$  has zero mean. Note that rescaling and shifting a variable has no effect on mutual information, so we can rewrite the information rate as

$$i = \lim_{dt \rightarrow 0} \frac{I[\mathbf{n}; \mathbf{z}]}{dt}. \quad (\text{E11})$$

We then rewrite the mutual information as a KL divergence and expand, obtaining

$$I[\mathbf{n}; \mathbf{z}] = \langle D_{\text{KL}}[p(\mathbf{z}|\mathbf{n}) \| p(\mathbf{z})] \rangle_{p(\mathbf{n})} \quad (\text{E12a})$$

$$= \langle D_{\text{KL}}[p(\mathbf{z}|\mathbf{n}) \| \tilde{p}(\mathbf{z})] \rangle_{p(\mathbf{n})} - D_{\text{KL}}[p(\mathbf{z}) \| \tilde{p}(\mathbf{z})]. \quad (\text{E12b})$$

Here we have defined

$$\tilde{p}(\mathbf{z}) := \mathcal{N}(0, 1_{d-1}). \quad (\text{E13})$$

The first term is straightforward to evaluate since it is a KL-divergence between two Gaussians with equal covariances, and yields

$$\langle D_{\text{KL}}[p(\mathbf{z}|\mathbf{n}) \| \tilde{p}(\mathbf{z})] \rangle_{p(\mathbf{n})} = \left\langle \frac{1}{2} |\langle \mathbf{z} \rangle_{p(\mathbf{z}|\mathbf{n})}|^2 \right\rangle_{p(\mathbf{n})} \quad (\text{E14a})$$

$$= \left\langle \frac{dt}{4D_c} |\boldsymbol{\mu}(\mathbf{n}) - \langle \boldsymbol{\mu} \rangle_{p(\mathbf{n})}|^2 \right\rangle_{p(\mathbf{n})} \quad (\text{E14b})$$

$$= \frac{dt}{4D_c} \text{Tr} [\text{Cov}(\boldsymbol{\mu})]. \quad (\text{E14c})$$

It then remains to evaluate the second term. Here we define  $\mathbf{m}(\mathbf{n}) = \langle \mathbf{z} \rangle_{p(\mathbf{z}|\mathbf{n})}$ , and note that it is proportional to  $\sqrt{dt}$  and thus small, then note that we can write the marginal distribution as

$$p(\mathbf{z}) = \langle \tilde{p}(\mathbf{z} - \mathbf{m}(\mathbf{n})) \rangle_{p(\mathbf{n})} \quad (\text{E15a})$$

$$= \left\langle \tilde{p}(\mathbf{z}) \left[ 1 + \mathbf{z} \cdot \mathbf{m}(\mathbf{n}) + \frac{1}{2} ([\mathbf{z} \cdot \mathbf{m}(\mathbf{n})]^2 - |\mathbf{m}(\mathbf{n})|^2) + \mathcal{O}(\mathbf{m}^3) \right] \right\rangle_{p(\mathbf{n})} \quad (\text{E15b})$$

$$= \tilde{p}(\mathbf{z}) \left[ 1 + 0 + \frac{1}{2} (\mathbf{z}^\top \Sigma_{\mathbf{m}} \mathbf{z} - \text{Tr} \Sigma_{\mathbf{m}}) + \mathcal{O}(dt^{3/2}) \right]. \quad (\text{E15c})$$

Here we expanded around  $\mathbf{m} = 0$ , and kept terms up to first order in  $dt$ . We can then evaluate the 2nd KL-divergence term by expanding the integrand around  $dt = 0$ , which yields

$$D_{\text{KL}}[p(\mathbf{z}) \| \tilde{p}(\mathbf{z})] = 0 + \frac{1}{2} \left[ \underbrace{\langle \mathbf{z}^\top \Sigma_{\mathbf{m}} \mathbf{z} \rangle_{\tilde{p}(\mathbf{z})}}_{\text{Tr} \Sigma_{\mathbf{m}}} - \text{Tr} \Sigma_{\mathbf{m}} \right] + \mathcal{O}(dt^{3/2}) = 0 + \mathcal{O}(dt^{3/2}). \quad (\text{E16})$$

Thus after dividing by  $dt$ , this contribution to the mutual information is negligible in the small- $dt$  limit. This concludes our proof, and we have

$$i = \frac{1}{4D_c} \text{Tr} [\text{Cov}(\boldsymbol{\mu})]. \quad (\text{E17})$$

### E.3 Continuous Steering in $d$ Dimensions

For continuous steering, we analytically obtain a near-optimal strategy in  $d$ -dimensions with “2D noise”. When signed information is available, we expect an equilibrium stationary distribution (from the dynamics given by Eq. (E6)) such that

$$\boldsymbol{\mu}(\mathbf{n}) = (D_r + D_c)\nabla \ln p(\mathbf{n}). \quad (\text{E18})$$

Analogous to the von-Mises ansatz in two dimensions, we consider a von-Mises-fisher ansatz here,

$$p(\mathbf{n}) = \frac{\kappa^{d/2-1}}{(2\pi)^{d/2} 1_{d/2-1}(\kappa)} \exp(\kappa \mathbf{r}^\top \mathbf{n}), \quad (\text{E19})$$

where  $\kappa$  is a shape parameter and  $\mathbf{r}$  is the target heading.

The generalization for the velocity is  $v/v_0 = \langle \mathbf{n} \cdot \mathbf{r} \rangle$ , which we can evaluate as

$$v/v_0 = \frac{1_{d/2}(\kappa)}{1_{d/2-1}(\kappa)}, \quad (\text{E20})$$

with  $I_m(x)$  denoting the  $m$ -th order modified Bessel function of the first kind. We can similarly evaluate the information rate, for which we obtain

$$i = \frac{1}{4D_c} \text{Tr}[\text{Cov}(\boldsymbol{\mu})], \quad (\text{E21})$$

which can be evaluated as

$$i/D_r = (d-1)\kappa \frac{1_{d/2}(\kappa)}{1_{d/2-1}(\kappa)}. \quad (\text{E22a})$$

Here we have taken  $D_c = D_r$ , which is optimal by the same arguments we used in two dimensions.

Combining these two results and eliminating  $\kappa$ , we obtain an analytic performance trade-off curve in arbitrary dimensions, which will be a lower bound on the optimal Pareto frontier:

$$v/v_0 = \frac{1_{d/2}\left(\frac{i/D_r}{(d-1)v/v_0}\right)}{1_{d/2-1}\left(\frac{i/D_r}{(d-1)v/v_0}\right)}. \quad (\text{E23})$$

Expanding in the low and high information limits this gives

$$v/v_0 \approx \begin{cases} \sqrt{\frac{i/D_r}{d(d-1)}} & i/D_r \ll 1, \\ 1 - \frac{(d-1)^2}{2i/D_r} & i/D_r \gg 1. \end{cases} \quad (\text{E24})$$

### E.4 Unsigned Steering in 3 Dimensions

We then turn to the question of how unsigned steering should be generalized to 3 dimensions. Consider the degree of deviation of the current heading  $\mathbf{n}$  from the target heading  $\mathbf{r}$ , which can be quantified by the angle  $\theta$  between them such that  $\mathbf{n} \cdot \mathbf{r} = \cos \theta$ . To parameterize  $\mathbf{n}$  we require two angles,  $\theta$  (the angle between the heading and the target), and  $\phi$  the perpendicular angle with respect to which we expect the problem to be symmetric. Now suppose that the strategy  $\boldsymbol{\mu}$  can only depend on the value of  $\mathbf{n} \cdot \mathbf{r}$ , or equivalently on  $\cos \theta$ . What is the optimal strategy under this constraint?

In two dimensions the agent was pinned to a plane, and could thus choose to steer left or right even without knowledge of which direction pointed towards the target direction. In three dimensions, however, this no longer makes sense, since the agent can roll freely around the heading vector  $\mathbf{n}$ . We thus treat the steering capabilities of the agent as applying a steering force in a vector direction  $\mathbf{f}$  which is perpendicular to  $\mathbf{n}$ , such that  $\boldsymbol{\mu} = \mathbf{f}g(\theta)$  for some scalar function  $g(\theta)$  which we require to be even.

To make progress, we define an additional “facing” vector  $\mathbf{f}$  which is perpendicular to  $\mathbf{n}$ , and is the direction in which the agent can steer. We will quantify  $\mathbf{f}$  using the angle  $\psi$  between  $\mathbf{f}$  and the optimal steering force direction.

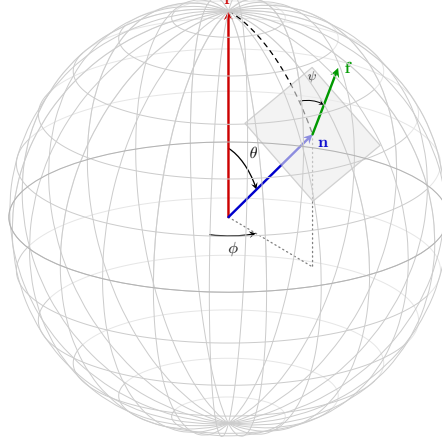


**Figure S6:** Schematic to illustrate the vectors and angles involved in 3D unsigned steering.

We would then write the steering force as  $\boldsymbol{\mu} = \mathbf{f} g(\theta)$ . We will describe the dynamics of this steering vector using the angle  $\psi$  between  $\mathbf{f}$  and the vector pointing directly towards the north pole. We assume this angle also undergoes rotational diffusion with a diffusion coefficient  $D_\psi$ . Figure S6 illustrates the geometry of the problem.

Carefully keeping track of the relevant geometric and trigonometric factors, we find that three angles in the problem evolve according to the following stochastic differential equations:

$$\dot{\theta} = -g(\theta) \cos \psi + \sqrt{2(D_c + D_r)} \eta_\theta(t), \quad (\text{E25a})$$

$$\dot{\phi} = -g(\theta) \sin \psi / \sin \theta + \frac{1}{\sin \theta} \sqrt{2(D_c + D_r)} \eta_\phi(t), \quad (\text{E25b})$$

$$\dot{\psi} = g(\theta) \sin \psi \cot \theta + \sqrt{2D_\psi} \eta_\psi(t). \quad (\text{E25c})$$

Here we have applied the controller noise  $D_c$  to both the  $\theta$  and  $\phi$  directions.

The associated Fokker-Planck equation is

$$\begin{aligned} \frac{\partial}{\partial t} p(\theta, \phi, \psi) = & -\frac{1}{\sin \theta} \partial_\theta [-g(\theta) \cos \psi \sin \theta p(\theta, \phi, \psi)] - \frac{1}{\sin \theta} \partial_\phi [-g(\theta) \sin \psi p(\theta, \phi, \psi)] \\ & - \partial_\psi [g(\theta) \cot \theta \sin \psi p(\theta, \phi, \psi)] + D_\psi \partial_\psi^2 p + (D_r + D_c) \left[ \frac{1}{\sin \theta} \partial_\theta (\sin \theta \partial_\theta p) + \frac{1}{\sin^2 \theta} \partial_\phi^2 p \right]. \end{aligned} \quad (\text{E26})$$

We then seek to optimize the objective

$$\mathcal{L} = \langle \cos \theta \rangle - \gamma \frac{1}{4D_c} \text{Tr} [\text{Cov}(\boldsymbol{\mu})] \quad (\text{E27})$$

with respect to  $D_c$  and the function  $g(x)$ .

We will derive the scaling in the low information limit using a series expansion. In the low information limit we have  $g_0 = 0$  and  $p_0 = 1/8\pi^2$ . We now expand around this limit in a small parameter  $\epsilon \propto 1/\gamma$ , as

$$p = \frac{1}{8\pi^2} + \epsilon p_1 + \mathcal{O}(\epsilon^2), \quad (\text{E28a})$$

$$g = 0 + \epsilon g_1(\theta) + \mathcal{O}(\epsilon^2). \quad (\text{E28b})$$

We require that  $g_1$  be an even function of  $\theta$ .

We will also assume  $p$  is independent of  $\phi$  so that the FPE can be simplified to

$$\frac{\partial}{\partial t} p(\theta, \psi) = -\frac{1}{\sin \theta} \partial_\theta [-g(\theta) \cos \psi \sin \theta p(\theta, \psi)] - \partial_\psi [g(\theta) \cot \theta \sin \psi p(\theta, \psi)] + D_\psi \partial_\psi^2 p + (D_r + D_c) \frac{1}{\sin \theta} \partial_\theta (\sin \theta \partial_\theta p). \quad (\text{E29})$$

At first order, we will have

$$\begin{aligned}
0 &= D_\psi \partial_\psi^2 p_1 + (D_r + D_c) \frac{1}{\sin \theta} \partial_\theta (\sin \theta \partial_\theta p_1) - \frac{1}{\sin \theta} \partial_\theta [-g_1 \cos \psi \sin \theta p_0] - \partial_\psi [g_1 \cot \theta \sin \psi p_0]. \\
&= D_\psi \partial_\psi^2 p_1 + (D_r + D_c) [\partial_\theta^2 p_1 + \cot \theta \partial_\theta p_1] + \cos \psi p_0 \partial_\theta g_1.
\end{aligned} \tag{E30}$$

This functional form strongly suggests the ansatz  $p_1(\theta, \psi) = T(\theta) \cos(\psi)$ . Any higher harmonics in  $\psi$  could exist transiently, but should decay to zero at steady state due to the  $\cos \psi$  forcing. This ansatz allows us to write

$$0 = -D_\psi \cos \psi T(\theta) + \cos \psi (D_r + D_c) [T''(\theta) + \cot \theta T'(\theta)] + \frac{1}{8\pi^2} \cos \psi g_1'(\theta). \tag{E31}$$

Dividing through by  $\cos \psi$  then gives an ODE for  $T(\theta)$ ,

$$0 = -D_\psi T(\theta) + (D_r + D_c) [T''(\theta) + \cot \theta T'(\theta)] + \frac{1}{8\pi^2} g_1'(\theta). \tag{E32}$$

We can then proceed to evaluate the velocity and information rate. We begin with the information rate, which is

$$\begin{aligned}
i &= \frac{1}{4D_c} \text{Tr} [\text{Cov}(\boldsymbol{\mu})] \\
&= \frac{1}{4D_c} \langle g^2 \rangle_{p(\theta, \phi, \psi)} \\
&= \frac{1}{4D_c} \int \int \int \epsilon^2 g_1(\theta)^2 p_0(\theta, \phi, \psi) \sin \theta d\theta d\phi d\psi + \mathcal{O}(\epsilon^3) \\
&= \frac{\epsilon^2}{8D_c} \int g_1(\theta)^2 \sin \theta d\theta + \mathcal{O}(\epsilon^3).
\end{aligned} \tag{E33}$$

Since  $\sin \theta > 0$  on  $(0, \pi)$ , so long as  $g_1$  is not identically zero for all  $\theta$  the information rate will be second order in  $\epsilon$ . We similarly evaluate the velocity as

$$\begin{aligned}
v/v_0 &= \langle \cos \theta \rangle \\
&= \epsilon \int \int \int \cos \theta p_1(\theta, \phi, \psi) \sin \theta d\theta d\phi d\psi + \mathcal{O}(\epsilon^2) \\
&= 2\pi\epsilon \left( \int \cos \psi d\psi \right) \left( \int T(\theta) \cos \theta \sin \theta d\theta \right) + \mathcal{O}(\epsilon^2) \\
&= 0 + \mathcal{O}(\epsilon^2).
\end{aligned} \tag{E34}$$

Unlike in two dimensions, the up-gradient velocity is exactly zero to first order in  $\epsilon$ , while the information rate is non-zero at second order in  $\epsilon$ . Thus  $v \sim \sqrt{i}$  scaling is impossible, and the low information velocity-information scaling can be at best  $v \sim i$ .